研究成果の刊行に関する一覧表

論文、総説等刊行物

1. Coban C, Igari Y, Yagi M, Reimer T, Koyama S, Aoshi T, Ohata K, Tsukui T, Takeshita F, Sakurai K, Ikegami T, Nakagawa A, Horii T, Nunez G, Ishii KJ*, Akira S* "Immunogenicity of whole parasite vaccines against *Plasmodium Falciparum* involves malarial hemozoin and host TLR9" ***Cell Host Microbe*** 2010; 7(1) p50-61
2. Koyama S, Aoshi T, Tanimoto T, Kumagai Y, Kobiyama K, Tougan T, Sakurai K, Coban C, Horii T, Akira S*, Ishii KJ*. Plasmacytoid dendritic cells delineate immunogenicity of influenza vaccine subtypes. ***Sci Transl Med***. 2010 2(25):25ra24.
3. Jounai N, Kobiyama K, Shiina M, Ogata K, Ishii KJ, Takeshita F. "NLRP4 Negatively Regulates Autophagic Processes through an Association with Beclin1." ***J Immunol.*** 2011 186(3):1646-55
4. Kuroda E, Ishii KJ, Uematsu S, Ohata K, Coban C, Akira S, Aritake K, Urade Y, Morimoto Y. "Silica crystals and aluminum salts regulate the production of prostaglandin in macrophages via NALP3 inflammasome-independent mechanisms." ***Immunity*** in press 2011
5. Fujimoto K, Karuppuchamy T, Takemura N, Shimohigoshi M, Machida T, Haseda Y, Aoshi T, Ishii KJ, Akira S, Uematsu S. "A new subset of CD103+CD8alpha+ DCs in the small intestine express TLR3, TLR7 and TLR9, and induce Th1 response and CTL activity" ***J. Immunol.*** In press 2011
6. Koyama S, Akira S and Ishii KJ. "Immune recognition of nucleic acids and their metabolites" Extra Nucleic Acids, edited by Kikuchi Y, Ryokova ET , ***Springer,*** 2010 (BOOK CHAPTER)
7. 小山正平、石井　健「粘膜アジュバント」**臨床粘膜免疫学**（清野宏編）2010 年 12 月 20 日発行　シナジー社
8. 鉄谷耕平、石井　健　「アジュヴァント小史」**臨床とウイルス**，38(5) ： 367-378，2010
9. 小山正平、石井　健　「ワクチンアジュバントの必要性と安全性」**医学のあゆみ**　(2010) 234(3):217-221. 2010
10. 青枝大貴、石井　健　「ワクチンを考えるうえで必要な免疫の知識」**臨床検査**　Vol. 54 No. 11 2010. 10. 30 増刊号
11. 小山正平、石井　健　「ウイルス感染予防に用いられるワクチンアジュバント」 **次世代ワクチンの産業応用技術**（神谷　齊監修）　シーエムシー出版 2010 年 9 月 30 日 p112-124
12. 小檜山康司、石井　健　「DNA センサーとその生理的意義」　**細胞工学**　Vol. 29 No. 10(2010. 9. 22) p1004-1013
13. 小檜山康司、石井　健　「自然免疫とワクチン開発」　**医学のあゆみ**　Vol. 234 No. 5(2010. 7. 31) p608-614
14. 小檜山康司、石井　健　「アジュバントに関する最新の話題」**臨床と微生物**　2010 年 5 月 37(3) 187-194

15. Okada K, Komiya T, Yamamoto A, Takahashi M, Kamachi K, Nakano T, Nagai T, Okabe N, Kamiya H, **Nakayama T.** Safe and effective booster immunization using DTaP in teenagers. Vaccine 28: 7626-7633, 2010
16. Sakata M, **Nakayama T.** Protease and helicase domains are related to the temperature sensitivity of wild-type rubella viruses. Vaccine 29: 1107-1113, 2011
17. Sawada A, Komase K, **Nakayama T.** AIK-C measles vaccine expressing fusion protein of respiratory syncytial virus induces protective antibodies in cotton rats. Vaccine 29: 1481-1490, 2011
18. Nochi T, Yuki Y, Takahashi H, Sawada S, Mejima M, Kohda T, Harada N, Kong IG, Sato A, Kataoka N, Tokuhara D, Kurokawa S, Takahashi Y, Tsukada H, Kozaki S, Akiyoshi K, **Kiyono H.** Nanogel antigenic protein-delivery system for adjuvant-free intranasal vaccines.***Nat Mater.*** 2010 9:572-8.
19. Tokuhara D, Yuki Y, Nochi T, Kodama T, Mejima M, Kurokawa S, Takahashi Y, Nanno M, Nakanishi U, Takaiwa F, Honda T, **Kiyono H**.Secretory IgA-mediated protection against V. cholerae and heat-labile enterotoxin-producing enterotoxigenic Escherichia coli by rice-based vaccine. ***Proc Natl Acad Sci U S A.*** 2010 107:8794-9.
20. Obata T, Goto Y, Kunisawa J, Sato S, Sakamoto M, Setoyama H, Matsuki T, Nonaka K, Shibata N, Gohda M, Kagiyama Y, Nochi T, Yuki Y, Fukuyama Y, Mukai A, Shinzaki S, Fujihashi K, Sasakawa C, Iijima H, Goto M, Umesaki Y, Benno Y, **Kiyono H**. Indigenous opportunistic bacteria inhabit mammalian gut-associated lymphoid tissues and share a mucosal antibody-mediated symbiosis. ***Proc Natl Acad Sci U S A.*** 2010 20;107:7419-24.
21. Ichinohe T, Ainai A, Ami Y, Nagata N, Iwata N, Kawaguchi A, Suzaki Y, Odagiri T, Tashiro M, Takahashi H, Strayer D, Carter W, Chiba J, Tamura S, Sata T, Kurata T, **Hasegawa H** Intranasal administration of adjuvant-combined vaccine protects monkeys from challenge with the highly pathogenic influenza A H5N1 virus ***Journal of Medical Virology,*** 2010 Oct;82(10):1754-61
22. **Sakoda Y**, Sugar S, Batchluun D, Erdene-Ochir TO, Okamatsu M, Isoda N, Soda K, Takakuwa H, Tsuda Y, Yamamoto N, Kishida N, Matsuno K, Nakayama E, Kajihara M, Yokoyama A, Takada A, Sodnomdarjaa R, Kida H. Characterization of H5N1 highly pathogenic avian influenza virus strains isolated from migratory waterfowl in Mongolia on the way back from the southern Asia to their northern territory. **Virology,** 406. 88-94. 2010

一般紙・業界紙・一般向け雑誌等への掲載、テレビ・新聞報道など

1. インフルエンザワクチンの作用機序解明に関する論文発表（Koyama S et al Science Translational Medicine 2010 2(25):25ra24.）に関し、ＭＳＮニュース、ＮＨＫ、日本経済新聞、共同通信、朝日新聞、産経新聞、時事通信、日経ＢＴＪなどで報道された。上記のうち朝日、日経、産経、日経産業新聞の記事を添付。
2. ワクチンフォーラム（共催）、ワクチンワークショップのチラシ

Cell Host & Microbe
Article

Immunogenicity of Whole-Parasite Vaccines against *Plasmodium falciparum* Involves Malarial Hemozoin and Host TLR9

Cevayir Coban,[1] Yoshikatsu Igari,[1,5] Masanori Yagi,[2] Thornik Reimer,[4] Shohei Koyama,[1] Taiki Aoshi,[2] Keiichi Ohata,[1,5] Toshihiro Tsukui,[5] Fumihiko Takeshita,[6] Kazuo Sakurai,[7] Takahisa Ikegami,[3] Atsushi Nakagawa,[3] Toshihiro Horii,[2] Gabriel Nuñez,[4] Ken J. Ishii,[1,2,*] and Shizuo Akira[1,*]

[1]Laboratory of Host Defense, WPI Immunology Frontier Research Center
[2]Department of Molecular Protozoology, Research Institute for Microbial Diseases
[3]Institute for Protein Research
Osaka University, Osaka 565-0871, Japan
[4]Department of Pathology and Comprehensive Cancer Center, The University of Michigan Medical School, Ann Arbor, MI 48109, USA
[5]ZENOAQ, Nippon Zenyaku Kogyo Co. Ltd., Fukushima 963-0196, Japan
[6]Department of Molecular Biodefense Research, Yokohama City University Graduate School of Medicine, Yokohama 236-0004, Japan
[7]Department of Chemical Processes & Environments, The University of Kitakyushu, Fukuoka 808-0135, Japan
*Correspondence: kenishii@biken.osaka-u.ac.jp (K.J.I.), sakira@biken.osaka-u.ac.jp (S.A.)
DOI 10.1016/j.chom.2009.12.003

SUMMARY

Although whole-parasite vaccine strategies for malaria infection have regained attention, their immunological mechanisms of action remain unclear. We find that immunization of mice with a crude blood stage extract of the malaria parasite *Plasmodium falciparum* elicits parasite antigen-specific immune responses via Toll-like receptor (TLR) 9 and that the malarial heme-detoxification byproduct, hemozoin (HZ), but not malarial DNA, produces a potent adjuvant effect. Malarial and synthetic (s)HZ bound TLR9 directly to induce conformational changes in the receptor. The adjuvant effect of sHZ depended on its method of synthesis and particle size. Although natural HZ acts as a TLR9 ligand, the adjuvant effects of synthetic HZ are independent of TLR9 or the NLRP3-inflammasome but are dependent on MyD88. The adjuvant function of sHZ was further validated in a canine antiallergen vaccine model. Thus, HZ can influence adaptive immune responses to malaria infection and may have therapeutic value in vaccine adjuvant development.

INTRODUCTION

Whole-microbe vaccines have been successful in preventing and/or treating many infectious diseases, by harboring not only protective antigens, but also "built-in" adjuvant components capable of activating the innate immune system (Pulendran and Ahmed, 2006; Ishii et al., 2008; Palm and Medzhitov, 2009). In the case of malaria, there is evidence that host protective immunity against blood stage malaria parasites can be achieved in humans as well as in animal models following whole-parasite vaccinations, although large numbers of parasites are required (Good, 2009; Doolan et al., 2009). Among parasite-derived molecules, potentially protective antigens have been investigated intensively for vaccine development (Girard et al., 2007; Coppel, 2009). However, the adjuvant components within blood stage parasites have not been explored; likely adjuvant components include ligands for innate immune receptors, such as Toll-like receptors (TLRs), NOD-like receptors (NLRs), and RIG-I-like receptors (Stevenson and Riley, 2004; Coban et al., 2007a).

There are several candidate molecules in Plasmodium parasites that could act as adjuvant components (Schofield et al., 2002; Pichyangkul et al., 2004; Krishnegowda et al., 2005; Coban et al., 2005; Parroche et al., 2007; Seixas et al., 2009). TLR2 and TLR9 have been shown to mediate innate immune system activation by GPI, a heat-labile fraction, and hemozoin (HZ) and DNA derived from *Plasmodium falciparum* (*Pf*) (Krishnegowda et al., 2005; Pichyangkul et al., 2004; Coban et al., 2005; Parroche et al., 2007); however, discrepancies among these findings remain unresolved (Coban et al., 2007a). TLR9 has also been proposed to play important roles in the pathogenesis of cerebral malaria by recruiting immune cells into the brain (Coban et al., 2007b; Griffith et al., 2007), or in that of severe malaria owing to the induction of regulatory T cells and/or synergy with interferon γ (IFNγ) signaling (Hisaeda et al., 2008; Franklin et al., 2009), but this is also controversial with some reports suggesting that this is not the case (Lepenies et al., 2008; Togbe et al., 2007). In addition, recent reports suggest that uric acid is released during malaria infection (Orengo et al., 2008), thereby activating the innate immune system presumably via NLRs, particularly NLRP3 (also known as NALP3) and its adaptor molecule apoptosis-associated speck-like protein containing a CARD domain (ASC), leading to caspase-1 activation (Franchi et al., 2009).

We therefore investigated further whether TLRs, and TLR9 in particular, as well as other innate immune receptors such as NLRs, are involved in *Pf*-mediated innate and adaptive immune responses, and whether HZ plays any role in such adaptive immune responses. We found that *Pf* whole-parasite crude

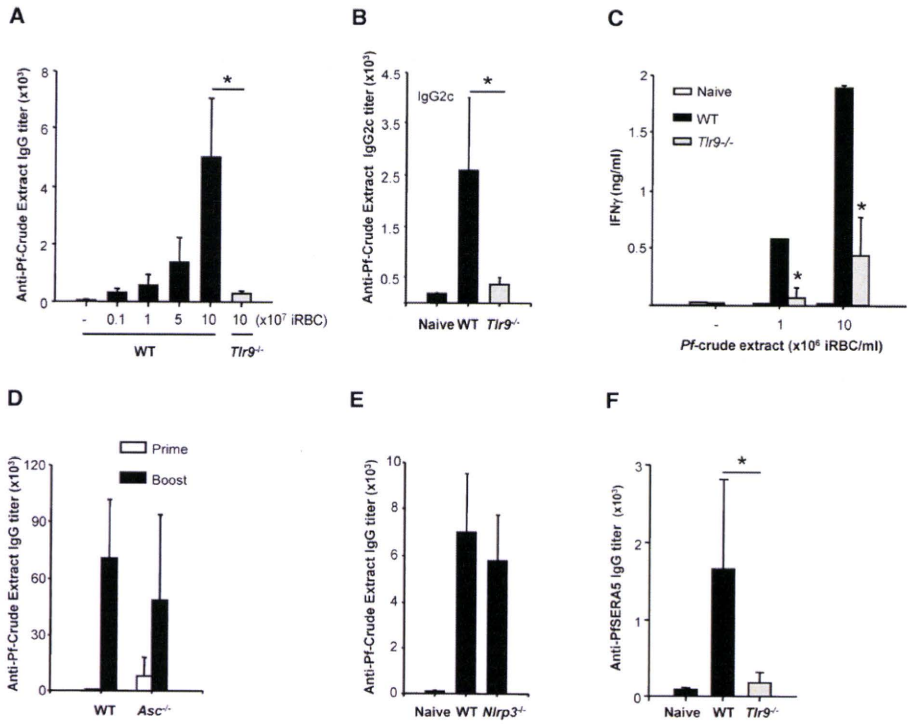

Figure 1. *Pf* Crude Extract Contains an Adjuvant Element for Coadministered Malaria Antigens in a TLR9-Dependent Manner

(A–C) Serum anti-*Pf* crude extract-specific IgG (A) and IgG2c antibody responses (B) and IFNγ from cultured spleen cells (C) were measured by ELISA at 3 weeks after the intraperitoneal immunizations with *Pf* crude extract. See also Figure S1.

(D and E) Serum anti-*Pf* crude extract-IgG antibody responses of *Nlrp3*$^{-/-}$ and *Asc*$^{-/-}$ mice. (E) shows levels only after prime immunization.

(F) Sera from WT and *Tlr9*$^{-/-}$ mice were analyzed for anti-*Pf* SERA5-specific IgG responses. The results shown are representative of at least two independent experiments with three to five mice per group. (*$p < 0.05$; mean levels of serum antibodies ± standard deviation [SD]).

extracts elicit parasite antigen-specific adaptive immune responses via TLR9, but not via NLRP3 or ASC. The malarial product HZ showed a potent adjuvant effect without any requirement for DNA. Further analysis at the molecular and atomic levels revealed that TLR9 binds to HZ directly and specifically, in a manner that depends on particular motifs and amino acid sequences, similar to its binding of CpG DNA, a well-known TLR9 ligand. A synthetic version of HZ also displayed a strong adjuvant effect; however, its optimal response was quite variable and dependent on its method of synthesis as well as its structural appearance.

RESULTS

A *Pf* Crude Extract Contains a TLR9 Ligand as a Built-in Adjuvant for Coadministered Malaria Antigens

To examine the possible adjuvant effects of whole parasites, we prepared a large quantity of whole-parasite antigens by freeze-thawing of *Pf*-infected red blood cells. The resulting extract, designated the *Pf* crude extract, contained products from both parasites and host red blood cells was immunized into mice. Three weeks after immunization, without any additional adjuvant, a significantly higher titer of serum *Pf* crude extract-specific immunoglobin G (IgG) was detected compared with the titers in naive mice and mice immunized with a normal red blood cell extract, in a dose-dependent manner (Figure 1A and data not shown). The antibody titers were 10 times higher after boost immunizations (Figure 1D).

We subsequently examined whether the immunogenicity of the whole-parasite vaccine was altered in the absence of TLR9, because TLR9 has been shown to mediate innate immune system activation by a heat-labile fraction, HZ and DNA derived from *Pf* (Coban et al., 2007a). Accordingly, mice lacking TLR9 showed significantly lower serum IgG (mainly IgG2c) responses and T-cell-specific IFNγ levels than wild-type mice (Figures 1A–1C). This TLR9-dependent adjuvant effect of whole-parasite antigens was specific for the immunizing *Pf* antigens, such as *Pf* SERA5 and *Pf* MSP1 (Figure 1F and data not shown). TLR9-dependent IgG responses were also observed for IgG2b and IgG3, but not for IgG1 (see Figures S1A–S1C available online). These data clearly demonstrate that *Pf* crude extract possesses a TLR9 ligand as a built-in adjuvant for coadministered malaria antigens.

The ASC-Inflammasome Is Not Involved in the Adjuvant Effect of *Pf* Crude Extract

We next investigated whether the inflammasome and its components were involved, given the fact that *Plasmodium* parasites grown in erythrocytes increase the concentration of uric acid, a known NLRP3 ligand that acts as a "danger signal" and

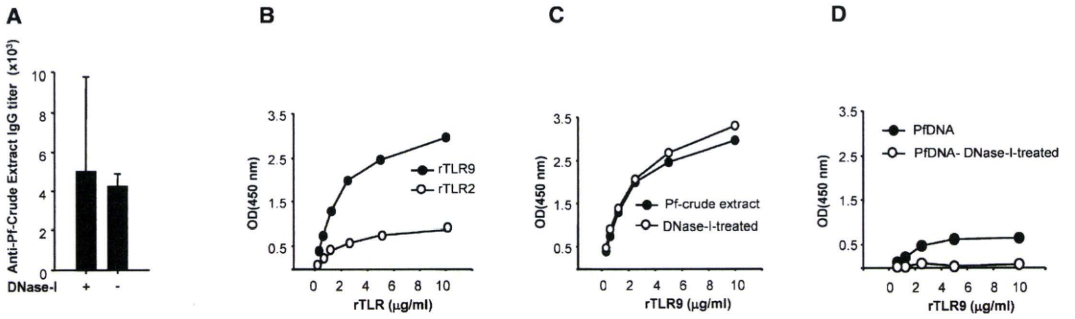

Figure 2. Malarial DNA Has No Role in the Adjuvanticity of *Pf* Crude Extract

(A) Serum anti-*Pf* crude extract-specific IgG antibody responses after immunization with DNase-I-treated and DNase-I-untreated *Pf* crude extracts. (n = 5 mice per group; mean ± SD). See also Figure S2B.

(B) Specific binding of rTLR2 or rTLR9 proteins to the coated *Pf* crude extract measured by ELISA. See also Figure S2A.

(C and D) Specific binding of rTLR9 protein to the coated DNase-I-treated or DNase-I-untreated *Pf* crude extract (C), or, to *Pf* DNA or DNase-I-treated *Pf* DNA (D). See also Figure S2B.

activates the ASC-inflammasome (Orengo et al., 2008). Moreover, recent studies suggest that DNA from any living organism may activate the ASC-inflammasome, independently of TLR9 (Muruve et al., 2008; Takeshita and Ishii, 2008), and that this may be mediated by AIM2 (Roberts et al., 2009; Hornung et al., 2009; Fernandes-Alnemri et al., 2009; Burckstummer et al., 2009). However, neither ASC- nor NLRP3-deficient mice showed any reduction in the adjuvant effect of *Pf* crude extract (Figures 1D and 1E). These data suggest that the critical adjuvant activity within *Pf* crude extract is mediated by TLR9, but not ASC-inflammasome.

Pf DNA Is Not Involved in the Adjuvant Effect of *Pf* Crude Extract

What components of the malaria parasite are responsible for the TLR9-dependent adjuvant effect? Although immune recognition of malarial HZ by TLR9 has been previously demonstrated in vitro and in vivo (Coban et al., 2005), another study suggested that HZ itself was immunologically inert, and that TLR9-dependent immune activation is instead caused by HZ-conjugated malarial DNA (Parroche et al., 2007). To investigate whether Plasmodium DNA is responsible for the TLR9-dependent adjuvant effect of *Pf* crude extract, DNA was removed by DNase-I treatment. To confirm that DNA was successfully removed from *Pf* crude extract, we performed *Pf* typing polymerase chain reaction (PCR) based on the nested PCR technique (Snounou et al., 1993), and did not find a trace of *Pf*DNA after DNase-treatment (Figure S2B). After immunizations, we found that the TLR9-dependent adjuvant effect of whole-parasite antigens was not affected by DNase-I treatment (Figure 2A), suggesting that DNA is not the TLR9-dependent adjuvant component of *Pf* crude extract.

A ligand is defined as a molecule with affinity and specificity for binding directly to a receptor. To examine such direct interactions between TLR9 and *Pf* crude extract, we established an enzyme-linked immunosorbent assay (ELISA)-based binding assay. Both rTLR9 and rTLR2 showed specific interactions with their cognate ligands (Figure S2A), confirming previous findings (Rutz et al., 2004). When the *Pf* crude extract was tested for binding to rTLR9 and rTLR2, we found that TLR9, and to a lesser extent TLR2, interacted strongly and in a dose-dependent manner with the *Pf* crude extract (Figure 2B), consistent with the findings of a previous report (Parroche et al., 2007). However, in sharp contrast with their findings, DNase-I treatment of the *Pf* crude extract did not alter its interaction with rTLR9, while the same DNase-I treatment abrogated TLR9 binding to *Pf* genomic DNA (Figures 2C and 2D). Of note, in contrast to the findings of Parroche et al., several attempts using nuclease treatment of *Pf* crude extract with several nuclease sources, showed either no effect on *Pf* crude extract binding to TLR9 or even nonspecific binding to TLR9 protein (Figures S2B and data not shown). Taken together, these data clearly demonstrate that some component of the *Pf* crude extract acts as a TLR9 ligand, mediates adaptive immune responses through TLR9, and directly binds to rTLR9 in a specific manner, and that this interaction does not require or involve DNA.

Hemozoin Binds Specifically to and Changes the Conformation of TLR9

After eliminating the possible involvement of genomic DNA in *Pf* crude extract adjuvanticity, we next investigated the role of hemozoin as a possible adjuvant molecule in the *Pf* crude extract. Given that it is not possible to deplete hemozoin from *Pf* crude extract without denaturing the malarial antigens (Figure S2C), and that using extensively purified natural *Pf*HZ would always be questioned on the basis of its purity, we used synthetic hemozoin derived from a highly pure source and thought to be identical to natural HZ (Pagola et al., 2000). Competition assays were then performed to investigate whether sHZ could block the binding of TLR9 protein to *Pf* crude extract. TLR9 binding to the coated *Pf* crude extract was measured in the presence of sHZ, CpG DNA (another known TLR9 ligand) or monosodium urate crystals (MSU). MSU crystals are insoluble immunostimulatory crystals that activate the innate immune system in a TLR9-independent manner (Martinon et al., 2006), because they form crystals that resemble sHZ in size and rod shape by surface electron microscopy (Figure S2E). TLR9 binding to the *Pf* crude extract was blocked by sHZ in a dose-dependent manner, as

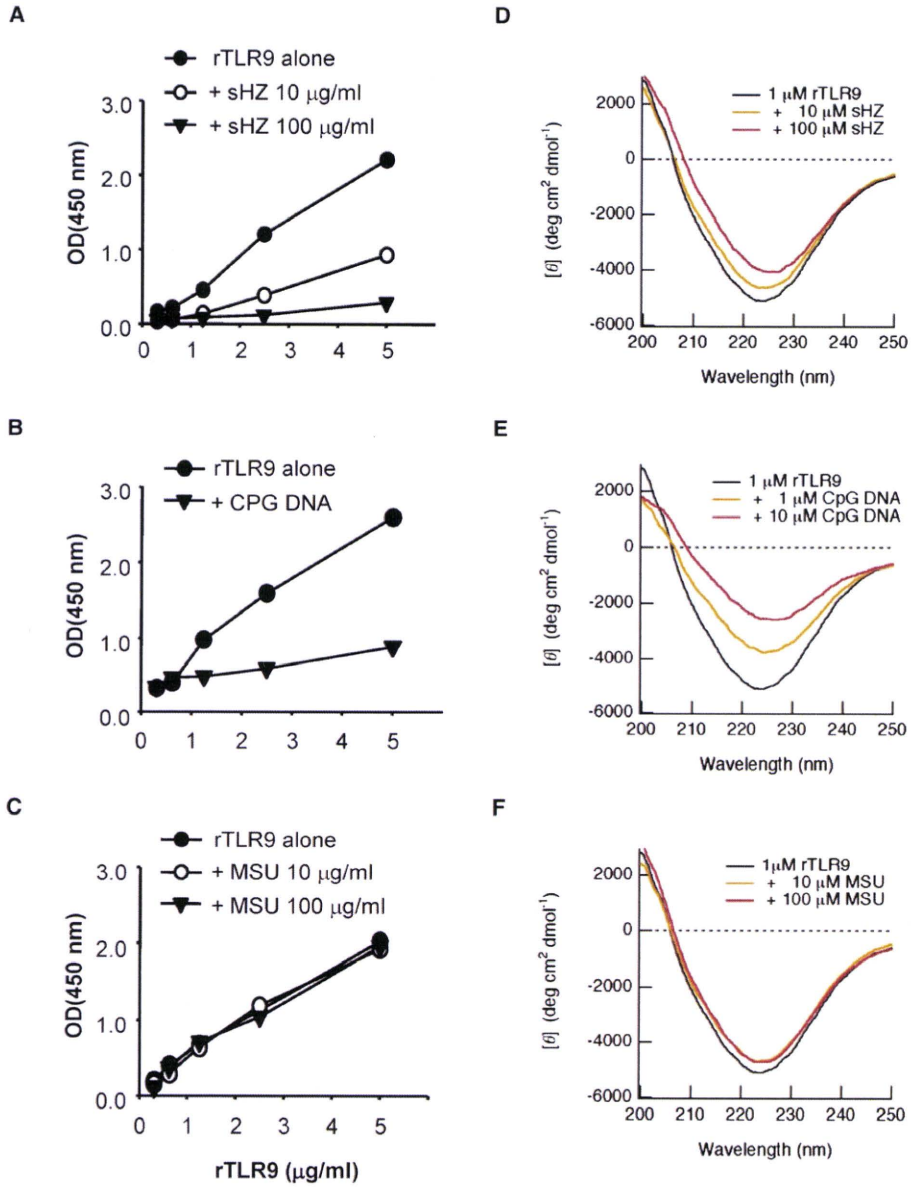

Figure 3. Synthetic Hemozoin Competes with *Pf* Crude Extract or CpG DNA for Binding to rTLR9 Protein

(A–C) Specific competition between the *Pf* crude extract and sHZ (A), CpG DNA (B) or MSU (C) was measured by ELISA.

(D–F) Conformational changes of rTLR9 protein were measured by CD in the presence and absence of sHZ (D), CpG DNA (E), or MSU (F). See also Figures S2C and S2F. All experiments were repeated at least five times with similar results.

well as CpG DNA (Figures 3A and 3B). On the other hand, MSU did not alter the binding of TLR9 to *Pf* crude extract (Figure 3C). Latz et al. recently demonstrated that TLR9 protein changes its conformation upon ligation (Latz et al., 2007). To monitor the conformational changes in the rTLR9 protein accompanying binding of its ligands, circular dichroism (CD) measurements were performed. Specifically, the CD spectra of rTLR9 protein were measured with or without the ligands at pH 5.5. The CD spectra of rTLR9 were altered by CpG DNA and sHZ, but not MSU, in a dose-dependent manner, characterized by remarkable spectral changes with shifts of the zero crossing point (Figures 3D–3F and Figure S2C). We also performed similar studies with soluble hemin that showed similar pattern and changed the conformation of rTLR9 as sHZ did, but not synthetic dsRNA (poly I:C) (Figure S2F). Taken together, these results demonstrate that sHZ can compete with *Pf* crude extract for binding to rTLR9 and change its conformation in a similar manner to CpG DNA.

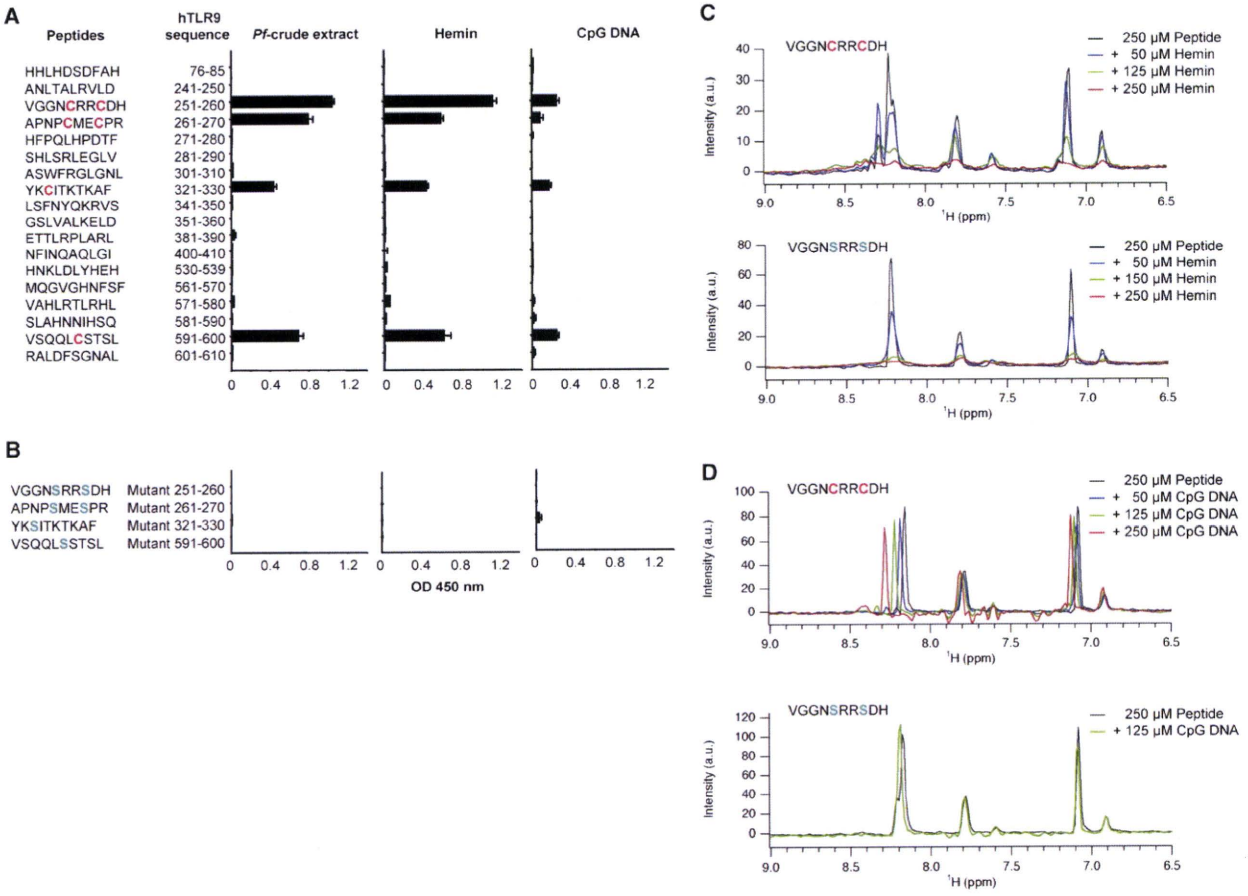

Figure 4. Peptide Regions in the Human TLR9 Sequence that Bind to *Pf* Crude Extract, Hemin, and CpG DNA

(A) Peptide sequences that are specific to human TLR9 extracellular domain and their binding to *Pf* crude extract, hemin and CpG DNA are investigated by ELISA.

(B) Binding of the peptides in which CysXXCys and Cys were respectively replaced with SerXXSer and Ser, as investigated by ELISA. Cys residues are labeled red, Ser residues are green.

(C and D) Interaction of the peptide VGGNCRRCDH and its mutant to various concentrations of hemin (C) or CpG DNA (D), as investigated by NMR titration. See also Figure S3. One-dimensional ^{1}H spectra of the peptides were obtained upon the addition of hemin or CpG DNA, and they are shown overlapped.

Direct and Specific Interaction between Hemozoin and TLR9 Observed at the Molecular and Atomic Levels

To further clarify the nature of the interaction between TLR9 and HZ, short peptides containing unique sequences of the TLR9 extracellular domain (sequences that are specific to the TLR9 extracellular domain and not contained in the extracellular domains of the other TLR family proteins) were synthesized and screened to identify the binding site(s) for TLR9 ligands. The peptides were subjected to ELISA-based binding assays with various TLR9 ligands, namely, *Pf* crude extract, hemin (a single unit of HZ) and CpG DNA (Figure 4A). Only four peptides, all of which had unique CysXXCys or Cys motifs similar to zinc finger motifs, bound to these ligands. Cysteine was required for the binding of these peptides as revealed by the same assays using mutant peptides (in which Cys was mutated to Ser) for which the binding ability was completely abrogated (Figure 4B). To analyze the binding sites in the peptides at an atomic level, nuclear magnetic resonance (NMR) titration was performed with peptides and CpG DNA and hemin. Using the peptide VGGNCRRCDH, which had the highest binding to the TLR9 ligands (Figure 4A), and its mutant peptide, the concentration of hemin and CpG DNA was increased stepwise and the spectral changes caused by hemin and CpG DNA were followed for each, as shown in Figures S3A and S3B and in greater detail in Figures 4C and 4D. Both hemin and CpG DNA shifted a peak at a ^{1}H resonance frequency of 8.2 ppm and slightly shifted at 7.1 and 7.8 ppm; all peaks were broadened to a lower intensity, upon addition of increasing concentrations of hemin, although no significant broadening was observed for CpG DNA (Figures 4C and 4D). When we performed the same titration experiments using the mutant peptides that lack Cys, we observed no such shifts (Figures 4C and 4D), although a decrease in intensity still remained upon increasing the concentration of hemin. These results indicate that TLR9 binds both HZ and CpG DNA and suggest that 4 cysteine residues may play an important role in the interaction between TLR9 and its ligands.

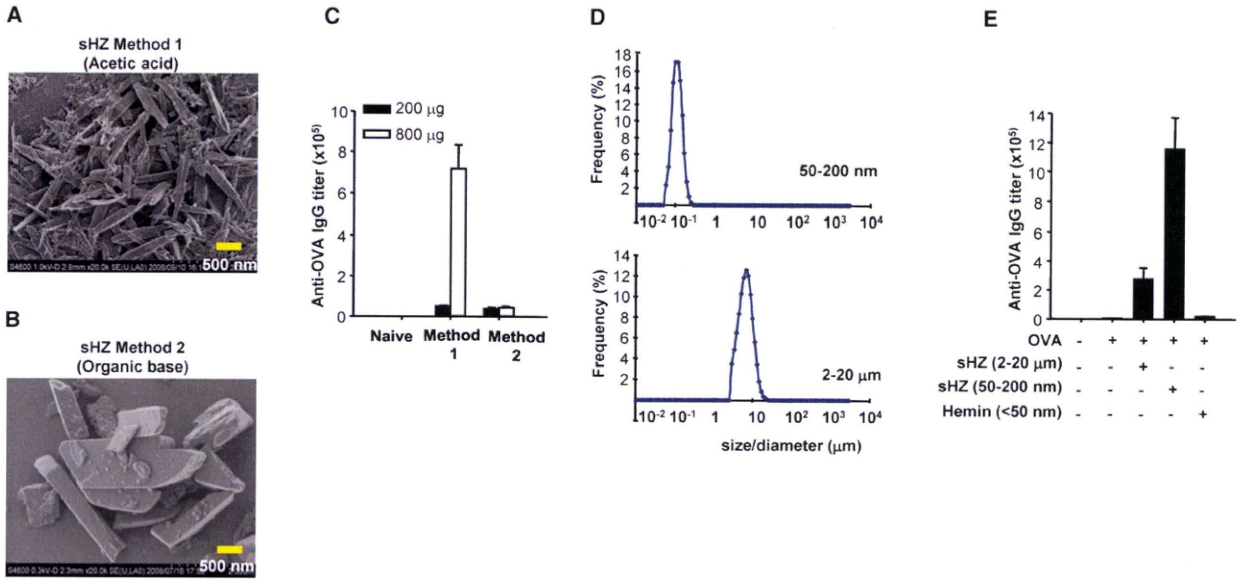

Figure 5. Adjuvanticity of Synthetic Hemozoin Crystals Depends on Their Size, with Smaller Crystals Showing a Better Adjuvant Effect

(A and B) FESEM images of sHZ synthesized by two different methods as described in Experimental Procedures. Scale bars, 500 nm.

(C) Serum OVA-specific IgG responses of C57B/6 mice s.c. immunized with OVA with or without sHZ purified by method 1 or method 2. See also Figure S4A–S4C.

(D) sHZ crystals produced by method 1 were size-differentiated using a laser-scattering particle size distribution analyzer.

(E) Mice were immunized to analyze the adjuvant effects of different sizes of sHZ (50–200 nm and 2–20 μm) and hemin (<50 nm). See also Figure S7. Results are representative of at least two independent experiments (mean ± SD; n = 3–5 mice per group).

Hemozoin Acts as a Potent Adjuvant, and Its Adjuvanticity Depends on Its Size

Is pure synthetic HZ a good adjuvant in vivo? Given the fact that various hemin chloride sources and methods can be used to synthesize sHZ, we first employed several production protocols to investigate the adjuvant properties of sHZ (Egan, 2008) using ultrapure hemin chloride. We found that two commonly used methods for synthesizing sHZ from hemin chloride produced crystals with a distinct appearance that differed in their adjuvant effects. With one method, HZ polymerized in the presence of acetic acid (method 1) and produced crystals that ranged in diameter from 50 nm to 1 μm, while the other method, involving an organic base (method 2), produced crystals that ranged in size from 1 to 5 μm as visualized by field emission scanning electron microscopy (FESEM) (Figures 5A and 5B). When mice were immunized with the model protein antigens ovalbumin (OVA) (or in some cases human serum albumin [HSA]) in the presence or absence of sHZ produced by method 1 or 2, the OVA-specific total IgG responses were significantly higher with sHZ produced by method 1 than with sHZ produced by method 2 (Figure 5C). Interestingly, when we separated the HZ produced by method 1 into two size distributions using a laser-scattering particle size distribution analyzer (Figure 5D), larger sHZ particles (up to 20 μm in size) were counted. It should be noted that sHZ crystals tend to make aggregates that the larger HZ particles might be attributed to the aggregation. Nevertheless, sHZ with sizes between 50 and 200 nm had optimal adjuvant effects compared with larger sHZ molecules (2–20 μm) and the smaller hemin monomer (<50 nm) (Figure 5E). We also examined different administration routes to investigate the adjuvant effects of sHZ such as subcutaneous (s.c.) and intranasal (i.n.) routes, and found that antigen-specific antibody responses were induced in a dose-dependent manner (Figures S4A and S4B and Figure 6A). There were no detectable OVA-specific IFNγ or interleukin (IL)-17 production by spleen cells, but substantial amounts of OVA-specific IL-13 and IL-5 were detected (Figure S4C). Analysis of the IgG isotypes elevated by sHZ coadministration showed that mainly IgG1 isotypes were elevated, followed by IgG2b and IgG2c, in mice (Figure 6B); this response was very potent when compared with those elicited by the adjuvants alum or CpG DNA (Figure 6C). On the other hand, sHZ administration elevated mainly IgG1 responses, while CpG DNA elevated mainly IgG2a (Figure S4D). Therefore, sHZ is indeed a potent adjuvant for protein vaccines, with optimal sizes of 20–200 nm, which coincide with the sizes of other particle adjuvants taken up by antigen-presenting cells via receptor-mediated endocytosis (McGee et al., 1997; Xiang et al., 2006).

Synthetic Hemozoin's Adjuvant Effect Is Mediated by MyD88, but Not TLR9 or the Inflammasome/IL-1β

We further investigated how the HZ adjuvant effect was regulated. To examine whether the potent adjuvant effect of sHZ was mediated by TLR9 and through MyD88, mice lacking TLR9 and MyD88 were immunized with OVA plus sHZ. MyD88-deficient mice failed to elicit a serum anti-OVA antibody titer (Figure 6D). By contrast, however, TLR9-deficient mice showed comparable anti-OVA titers to those in wild-type mice, suggesting that there are distinct mechanisms for the adjuvant effects of sHZ other than TLR9, any of which seem to culminate in

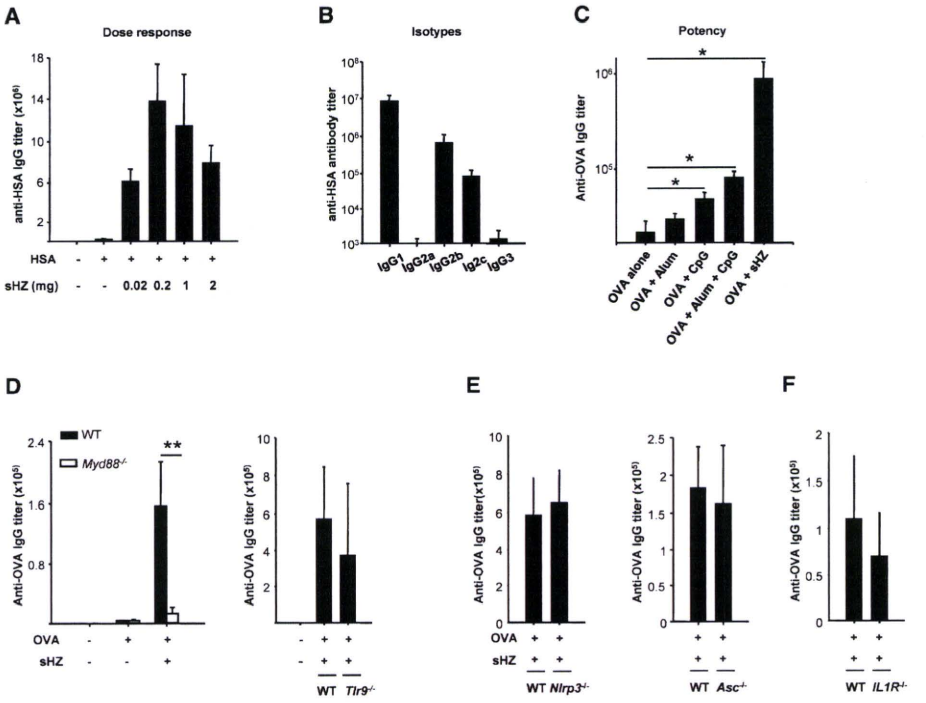

Figure 6. Synthetic Hemozoin's Potent Adjuvant Effect Is Mediated by MyD88 but Independently of TLR9 and the Inflammasome

(A and B) Mice were immunized with HSA and various concentrations of sHZ. Serum HSA-specific IgG (A) and IgG isotypes (B) were measured by ELISA (mean ± SD).

(C) Comparison of the adjuvant effects of alum, CpG DNA, and sHZ. Balb/c mice were immunized s.c. with OVA and alum (200 μg), CpG DNA (50 μg), and sHZ (800 μg), and serum OVA-specific IgG responses were determined after boost immunizations by ELISA (mean ± standard error; n = 3). *$p < 0.05$ compared with OVA-alone group. See also Figure S4D.

(D–F) Serum OVA-specific IgG responses of *Myd88*$^{-/-}$ and *Tlr9*$^{-/-}$ mice (D), *Nlrp3*$^{-/-}$ and *Asc*$^{-/-}$ mice (E), and *IL1R*$^{-/-}$ mice (F) after boost immunizations were determined by ELISA (**$p < 0.01$; mean ± SD). Wild-type (n = 5–6); *Myd88*$^{-/-}$ (n = 6); *TLR9*$^{-/-}$ (n = 6); *Nlrp3*$^{-/-}$ (n = 3); *Asc*$^{-/-}$ (n = 6) and *IL1R*$^{-/-}$ (n = 5). See also Figures S5A–S5C and Figure S6. Experiments are representative of at least two independent experiments.

MyD88-dependent signals. We confirmed these findings by obtaining similar results with HSA (Figures S5A and S5B).

Particles like MSU crystals have recently been shown to be recognized by NOD-like receptors (NLRP3 in the case of MSU) and form large cytosolic complexes, collectively called the inflammasome. We were interested in clarifying whether the adjuvanticity of sHZ, whose appearance resembles MSU crystals (Figure 5A and Figure S2D), could involve the inflammasome. In the same set of OVA or HSA immunization protocols, mice deficient in ASC or NLRP3 elicited normal antibody responses (Figure 6E and Figure S5B) as well as IL1R-deficient mice (Figure 6F and Figure S5C). These results suggest that inflammasome/ IL-1β pathway have a minimal role in the adjuvant effect of sHZ.

To examine whether sHZ-induced inflammation occurs in vivo, we measured neutrophil recruitment. When sHZ was injected intraperitoneally, significant numbers of neutrophils were recruited into the peritoneum within 24 hr (Figure S6A), and the neutrophil recruitment occurred normally in mice lacking either ASC or TLR9 (Figure S6B). However, mice lacking MyD88 failed to exhibit neutrophil recruitment in response to sHZ injection (Figure S6A).

Synthetic Hemozoin Is a Potent Adjuvant for Malarial Antigens as Well as for an Allergen

It has been previously shown that subclinical infection of healthy human volunteers with red cells infected with *Pf* or immunization of mice with a small number of dead parasites in the presence of CpG DNA or alum can induce cellular immunity and protection (Pombo et al., 2002; Good, 2009). To examine whether sHZ would have a potent adjuvant effect on immunization with *Pf* crude extract from a few parasites, we immunized mice s.c. with 10 μg total *Pf* crude extract together with sHZ, boosted twice, and measured anti-*Pf* crude extract specific antibody responses. sHZ significantly improved IgG levels (mainly IgG2c and IgG1) against *Pf* crude extract (Figure 7A and data not shown).

To examine whether sHZ could be used in animal species other than mice, we immunized Beagle dogs with house dust mite allergen (Derf2) together with alum and sHZ, and boosted that elevated IgG2 type (but not IgG1) antibodies, which may resemble Th1-like immune responses in dogs (Figure 7B and 7C) (Hou et al., 2006). Accordingly, Derf2-specific IgE responses after Ag challenges were significantly reduced in sHZ coadministered dogs (Figure 7C). It is of note, however, that antibody

responses elicited in mice were dominant with IgG1 isotype, which was different from those in dogs (Figure S5D). These data further suggest that sHZ may serve as a potent Th1-like adjuvant, at least in the canine model, while it acts like a Th2-dominant adjuvant in a murine model.

DISCUSSION

Malaria is still one of the leading pathogens, affecting 40% of the world's population and killing over one million people each year, but a successful vaccine against it not yet available. Owing to the failure of many clinical trials for recombinant vaccines, and recent progress in our understanding of innate immune adjuvant effect of microbial products (Kaisho and Akira, 2002), the whole-parasite vaccine strategy has been regaining attention (Good, 2009; Doolan et al., 2009). Successful vaccination with erythrocytic parasites was achieved using powerful adjuvants, such as CpG DNA (Su et al., 2003). We further demonstrated that an increased dose of a crude extract of *Pf* parasites without adjuvant successfully displayed strong immunogenicity, owing to the enhanced "built-in adjuvant" activity of the parasite. Surprisingly, this adjuvant effect was heavily dependent on TLR9. Because this has been a matter of controversy, the TLR9 ligand in malaria parasite was carefully analyzed again, and we found that DNA is not required for this TLR9-mediated adjuvant effect of the *Pf* crude extract (Figure 2). It is thus reasonable to interpret that the built-in adjuvant in *Pf* crude extract is a non-DNA TLR9 ligand, such as HZ and/or some other heat-labile components as previously reported (Coban et al., 2005; Pichyangkul et al., 2004).

HZ is a heme crystalline dimer generated by parasite digestion of hemoglobin as a byproduct of the heme detoxification system in malaria infection (Arese and Schwarzer, 1997; Hanscheid et al., 2007). It has been proposed to play important roles in pathophysiology during malaria infection, because it activates macrophages and dendritic cells to produce both proinflammatory and anti-inflammatory cytokines and chemokines (Engwerda and Good, 2005; Keller et al., 2006; Hanscheid et al., 2007; Coban et al., 2007a). Although immune recognition of malarial HZ by TLR9 has been demonstrated in vitro and in vivo (Coban et al., 2005), another study suggested that HZ itself was immunologically inert, and that TLR9-dependent immune activation is instead caused by HZ-conjugated malarial DNA (Parroche et al., 2007).

Parroche et al. suggested that DNase-I treatment of *Pf* crude extract did not remove *Plasmodium* DNA from *Pf*HZ shown by *Pf*-specific PCR (Parroche et al., 2007). When we performed PCR by using the same *Pf*-specific primers, 205 bp PCR product of *Pf* DNA was completely lost after DNase-I treatment (Figure S2B). We further confirmed the absence of *Pf* DNA after treatment of *Pf* crude extract by PCR using the other primers (101 bp product) (data not shown). In vivo, this DNase-free *Pf* crude extract displayed potent adjuvant activity via TLR9 (Figure 2A), strongly suggesting that the built-in adjuvant of *Pf* crude extract is not DNA.

What in *Pf* crude extract would be a TLR9 ligand rather than *Pf* DNA? We went on to reconfirm our previous finding that HZ is a TLR9 ligand by examining the definition of a ligand for a receptor, in which a ligand is to directly bind to a receptor in a specific manner. TLR9 binds directly both HZ and hemin, and change its conformation following binding to HZ (Figure 3). Moreover, competition for TLR9 binding occurs among *Pf* crude extract, CpG DNA, and sHZ, further supporting the possibility that HZ fulfills the definition of TLR9 ligand specificity. We also identified the binding motifs in the extracellular domain of TLR9, where cysteine residues play a crucial role in controlling the binding to ligands including *Pf* crude extract, heme, and CpG DNA (Figure 4). Taken together, these findings suggest that the adjuvant component of erythrocytic stage *Pf* parasites contains a TLR9 ligand, most likely HZ, but not DNA.

Involvement of the inflammasome pathways in inflammation during malaria infection, as has been implicated by a recent report (Orengo et al., 2008), was not apparent in the built-in adjuvant effect of whole-parasite vaccination with erythrocytic stage *Pf* crude extract (Figure 1). Consistently, the effect of synthetic HZ was also independent of the NLRP3-ASC inflammasome, as well as IL-1 receptor. It is of note that, while natural HZ in the *Pf* crude extract acts mostly as a TLR9 ligand, sHZ has an adjuvant effect independent of TLR9, but still utilizes the MyD88-dependent pathway. One possible explanation for this difference is that the uptake or ability to break the integrity of phagosomal and/or endosomal membrane of natural and synthetic HZ might differ given that the natural HZ is often covered by *Pf*-derived lipid, protein, or nucleic acids, compared with sHZ as a naked sharp crystal. Another explanation is that, although natural HZ purified from *Pf* cultures is known to be identical to sHZ (Pagola et al., 2000), several purification protocols give different crystal sizes ranging from 50 nm to 20 μm, which displayed quite different adjuvant activities (Figure 5). The studies are under investigation to examine whether different sizes of sHZ make distinct delivery and interaction with the innate immune cells and their immune receptors.

In addition, recent reports have suggested that immune recognition of and inflammatory response by sHZ is mediated by NLRP3 (Dostert et al., 2009; Griffith et al., 2009; Jaramillo et al., 2009). Although all of these three reports showed that IL-1β production by macrophages as well as neutrophil recruitment in response to sHZ was reduced in mice lacking NLRP3, precise mechanism of NLRP3-inflammasome activation are yet unclear. Griffith et al. suggested that uric acid is induced by sHZ and that the uric acid is the NLRP3 ligand (Griffith et al., 2009), but Dostert et al. suggested that uric acid is not involved in NLRP3 activation by sHZ (Dostert et al., 2009). Moreover, Jaramillo et al. showed elegantly that sHZ activates Lyn/Syk-mediated intracellular signaling pathway at the upstream of NLRP3 or ASC, indicating the existence of other HZ receptor(s) such as Dectin1, TREM family members, Siglec, or DAP12 (Jaramillo et al., 2009). Although the involvement of NLRP3 in sHZ-induced IL-1β or the following inflammatory response may play an important role in pathogenesis of malaria infections, we clearly demonstrate that NLRP3 as well as ASC, IL-1 receptor is not involved in sHZ-adjuvant activity (Figure 6), suggesting that there may be additional receptor(s) as well as pathway(s) for HZ-induced innate and adaptive immune activations.

Finally we found that sHZ acts as a potent adjuvant only when its synthesis method and size were optimized (Figure 5). This adjuvant effect of HZ for protein vaccines was observed with different model antigens, such as OVA and HSA, and via different

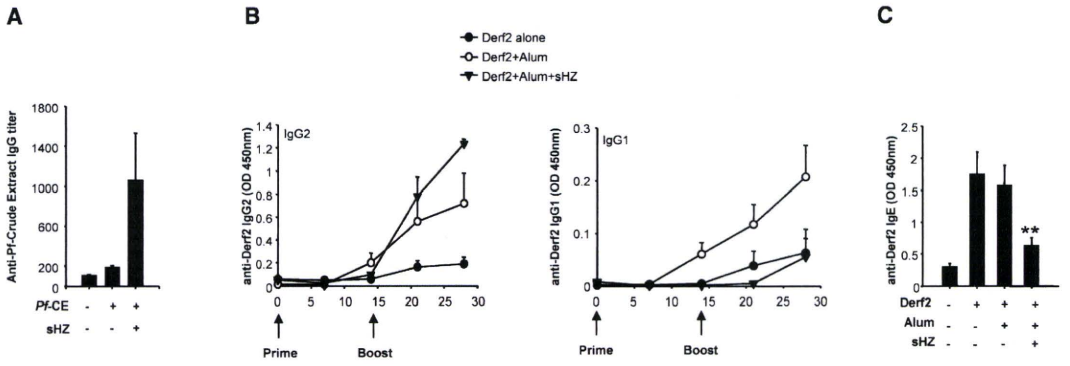

Figure 7. Synthetic Hemozoin Could Be Used as Adjuvant for Whole-Blood Malaria Antigens and Against Canine Allergy

(A) WT mice were immunized s.c. with 10 μg *Pf* crude extract and sHZ and were boosted twice. Serum *Pf* crude extract-specific IgG responses were analyzed by ELISA (mean ± SD; n = 4 per group).

(B and C) ELISA serum anti-Derf2-specific IgG2, IgG1 (B), and IgE (C) responses of Beagle dogs immunized with Derf2 antigen formulated with or without alum and alum + sHZ. See also Figure S5D. Experiments were repeated twice using four animals per group (**$p < 0.01$).

immunization routes, such as s.c. and i.n. immunization. It is of note that unlike CpG DNA, which has species-specific activity, HZ displayed its adjuvant effect in several animal models for vaccines, including murine, canine and non-human primate models (Figures 5–7, data not shown). In mice, a predominantly IgG1-dominant antibody adjuvant effect observed after HZ-adjuvanted immunization and T cell specific immune responses were mainly IL-13 and IL-5, but not IFNγ or IL-17, suggesting that HZ elicits Th2-type immune responses in mice (Figures 5, 6, and S4). However, by contrast, dog immunization with HZ elicited IgG2-dominant antibody responses, which is considered a Th1-type immune response (Reed and Scott, 1993). sHZ administration in the dog-allergy model was nonetheless very potent to reduce allergen-specific IgE responses (Figure 7), suggesting successful usage of sHZ as an adjuvant in dogs against allergy. Similarly, our data suggested that sHZ could be introduced externally as an adjuvant to improve immunogenicity of whole-malaria vaccines (Figure 7A). Our preliminary data also suggest that, in non-human primates, sHZ could elevate malarial antigen-specific B and T cell responses, and could be used as a vaccine adjuvant for whole-blood stage vaccines (K.J.I., unpublished data). Overall, our results clearly show that HZ possesses inflammatory and adjuvant activities through differential regulation by TLR9 pathways, thereby potentiating its ability to act as a therapeutic target for treating malaria infection, and its usefulness in vaccine adjuvant development.

EXPERIMENTAL PROCEDURES

Reagents

Hemin chloride was from Fluka (HPLC purified, >98% pure), whereas OVA and HSA (low endotoxin) were from Sigma. A synthetic CpG DNA (D35) was from Gene Design Incorporation. DNase-I was from Invitrogen. Zymosan was from Invivogen. MSU crystals were prepared as described elsewhere (Martinon et al., 2006).

Mice and Immunizations

Mice deficient for *MyD88*, *TLR9*, *Asc* or *Nlrp3*, and *Asc* on a C57BL/6 background were generated and used for experiments as described previously (Coban et al., 2005; Franchi and Nunez, 2008). All animal experiments were performed according to the institutional guidelines approved by the Research Institute for Microbial Diseases and Immunology Frontier Research Center of Osaka University and the University of Michigan.

Wild-type and *Tlr9*$^{-/-}$ mice were immunized intraperitoneally with the *Pf* crude extract (100 μl, approximately ~1 × 10^8 parasites). Alternatively, mice were immunized with a DNase-I-treated *Pf* crude extract. At 3 weeks after immunization, antibodies against *Pf* crude extract antigens in the sera of mice were detected by ELISA.

Various immunization schedules were conducted using either OVA or HSA as antigens. For s.c. immunizations, mice were injected on day 0 with 50 μg OVA (or 10 μg HSA) in a total of 200 μl sHZ solution at various concentrations and boosted on day 10 with 25 μg OVA (or 10 μg HSA) in the same sHZ solution. Blood samples were collected from the mice on day 17 for analysis of OVA- or HSA-specific antibody responses. For i.n. immunizations, mice were anesthetized and administered i.n. with 5 μg OVA with or without 80 μg sHZ (15 μl/nose), twice, at 2-week intervals. The mice were sacrificed 10 days after the boost, and serum, bronchoalveolar lavage fluid, and nasal fluid secretion samples were collected for antibody measurements.

Dogs and Allergy Model

Five-month-old Beagle dogs from the breeding colony at Zenoaq Animal Experiment Center (Nippon Zenyaku Kogyo Co., Ltd., Fukushima, Japan) were used. All immunization and sensitization protocols were performed in accordance with the institutional guidelines of and approved by Zenoaq Animal Center Laboratories Committee. Dogs were immunized s.c. on day 0 with 100 μg Derf2 protein produced in silkworms by a recombinant Baculovirus system, formulated in 500 μg aluminum hydroxide in a 200 μg sHZ solution, and boosted on day 14 with the same dose. Four weeks after the boost immunization, dogs were challenged with Derf2 s.c. four times biweekly. Blood samples were collected on days 7, 14, 21, and 28 for analysis of Derf2-specific IgG1 and IgG2 antibody responses, and on day 90 for the measurement of antigen-specific IgE responses.

Preparation of *Pf* Crude Extract, Natural HZ, Synthetic HZ, and *Pf* DNA

Mycoplasma-free *Pf* parasites (3D7) were maintained in culture medium as described previously (Aoki et al., 2002). After synchronization, mature and HZ-rich mostly trophozoite and schizont stage parasites (~4%–5%) were purified by 63% Percoll density centrifugation, washed and resuspended in incomplete medium, freeze-thawed three or four times, and stored at −80°C until use. Each milliliter of HZ-rich *Pf* crude extract preparation contained approximately 1 × 10^9 infected erythrocytes. As controls, uninfected human erythrocytes were treated similarly. Pure natural HZ was extensively purified from *Pf*-infected erythrocytes as described previously (Coban et al., 2005).

sHZ was purified from hemin chloride using two alternative methods (Egan, 2008). Method 1 (acid-catalyzed method) is known to produce smaller and homogenous crystals and was performed as previously described (Coban et al., 2005; Jaramillo et al., 2005). Briefly, 45 mg hemin chloride was dissolved in 4.5 ml 1 N NaOH and neutralized with 1 N HCl. Then, acetic acid was added until the pH reached 4.8, at a constant temperature of 60°C with magnetic stirring. The mixture was allowed to precipitate at room temperature overnight. The precipitate was subjected to washes with 2% SDS-buffered with 0.1 M sodium bicarbonate (pH 9.1) and subsequent extensive washes with 2% SDS, and then six to eight washes with distilled water. Method 2 (anhydrous method in methanol) is known to produce much bigger crystals and was performed as previously described (Bohle et al., 2002). Briefly, hemin chloride (52.2 mg) was dissolved completely in 2 ml 2,6-lutidine L, diluted with 10 ml dimethyl sulfoxide:methanol (1:1 mixture), tightly wrapped with parafilm and left at room temperature for 2 weeks in the dark, before being centrifuged and washed with 10 ml 0.1 M $NaHCO_3$ for 3 hr. The final product was washed three times with water and methanol, and dried. A stock solution in distilled water was prepared for use in in vivo studies and stored at 4°C. The HZ concentration was calculated as either mM or mg/ml after weighing the dried amount of sHZ. Experiments were mostly performed with sHZ prepared by method 1, except for the results shown in Figure 5B. All solutions were prepared and resuspended in endotoxin-free water (double-processed tissue culture water, Sigma-W3500) and stored in the dark at 4°C. There was no detectable level of endotoxin by LAL assay in any HZ preparation. None of the sHZ purified had any other contaminants, such as hemin, as determined by TLC (Figure S7A) or protein/DNA determined by SDS-PAGE at pH 11 and agarose gel, respectively (data not shown). FT-IR and powder X-ray diffraction pattern of the sHZ confirmed that the sample showed the same unit cell parameters as reported previously (Pagola et al., 2000) (Figures S7B and S7C). *Pf* genomic DNA was isolated as reported previously (Kongkasuriyachai et al., 2004).

Recombinant TLR Proteins and Peptides

Recombinant fusion proteins consisting of the extracellular domains of the human TLRs TLR9 (amino acids 1–818) and TLR2 (amino acids 1–588) fused to mouse IgG2b-Fc were constructed by amplifying the corresponding extracellular domain and ligating the fragment in frame into a pCIneo vector containing the coding sequence for mouse IgG2b-Fc. Fusion proteins were stably expressed in 293-F cells and purified from cell lysates by protein G affinity chromatography. Peptides were derived from unique regions of human *Tlr9* ectodomain sequence and synthesized by Operon Technologies.

Intraperitoneal Neutrophil Recruitment

sHZ (1000 μg) was resuspended in 200 μl PBS and intraperitoneally administered to various mice. At 16–18 hr after injection, the peritoneum was washed with a 30 ml cold PBS containing EDTA (3 mM) and heparin (10 U/ml) and the cells were counted. Neutrophils were identified using PE-conjugated anti-Gr-1 and APC-conjugated anti-CD11b antibodies (Becton Dickinson) in the presence of an anti-CD16 antibody. The stained cells were washed and analyzed using a FACSCalibur system.

Antibody and Cytokine ELISA

The plates were coated with OVA (1 μg/ml) or HSA (10 μg/ml), Derf2 (1 μg/ml) or *Pf* SE36 antigen (3 μg/ml) and analyzed by ELISA using a previously described procedure (Coban et al., 2005; Okech et al., 2006).

Spleens were extracted 3 weeks after the prime immunization and then stimulated with *Pf* crude extract. Seventy-two hours later, the cell culture supernatants were collected and analyzed for IFNγ, IL-13, IL-5, and IL-17 by ELISA (DuoSet ELISA Kit, R&D Systems).

Binding Assay and ELISA

Zymosan (5 μg/ml), CpG DNA (D35; 10 μg/ml), *Pf* crude extract (10 μg/ml), and *Pf* DNA (2 μg/ml) were coated on 96-well plates in PBS overnight at 4°C and then blocked with PBS containing 1% bovine serum albumin. The binding of TLR9 or TLR2 fusion proteins was detected with HRP-labeled mouse anti-IgG (Southern Biotech.). For competition ELISAs, rTLR9 protein was incubated with sHZ, MSU or CpG DNA for 1 hr and then incubated on *Pf* crude extract-coated plates for an additional 1 hr.

CD Spectroscopy

CD spectra were recorded with a J-820 spectropolarimeter (Jasco) using a 1 mm cell at 20°C. Each sample containing 1 μM TLR9 protein with or without a ligand (1 or 10 μM CpG DNA; 10 or 100 μM sHZ, or 10 or 100 μM MSU), was prepared in 20 mM sodium acetate buffer containing 150 mM NaCl at pH 5.5. Twenty spectra were acquired for each sample with a 1 nm bandwidth, a scanning speed of 50 nm per min, and a response time of 2 s, and then averaged. The resultant spectra were calculated after the spectra of rTLR9 were subtracted.

NMR Spectroscopy

^{1}H-1D NMR measurements were carried out using an AV400M NMR machine (Bruker BioSpin, Rheinstetten, Germany) with a 5 mm Shigemi tube (Shigemi, Tokyo, Japan) at 25°C. Each sample was prepared at a peptide concentration of 250 μM in 20 mM sodium phosphate buffer (pH 7.0) containing 10% (v/v) D_2O for the signal lock. For the measurements with hemin, various concentrations of hemin were prepared and the pH was set to 7.0 to prevent precipitation of hemin. For the measurements with CpG DNA (D35), because the signals from CpG DNA were larger than those from the peptides, the spectrum of D35 was subtracted from the spectra of the peptide-CpG DNA mixture to more easily judge the difference. All NMR data were processed and analyzed using NMRPipe (Delaglio et al., 1995) and Igor Pro (WaveMetrics, Lake Oswego, OR).

FESEM and Particle Size Analysis

Slides were coated with different dilutions of sHZ and images were captured using ultra-high-resolution FESEM (S-4800; Hitachi). The particle size and distribution in the sHZ solution were analyzed using a laser-scattering particle size distribution analyzer (LA-950; Horiba).

Statistical Analysis

Statistical differences between groups were analyzed using the Student's t test.

SUPPLEMENTAL INFORMATION

Supplemental Information includes seven figures and can be found with this article online at doi:10.1016/j.chom.2009.12.003.

ACKNOWLEDGMENTS

The authors sincerely thank Drs. N. Palacpac, T. Kanneganti, R. Jerala, M. Treeby, H. Kumar, and Y. Kumagai as well as the other members of Akira Lab and Horii Lab for their comments and for providing reagents, and Drs. S. Takahashi, T. Inoue, T. Inui, Y. Hara, Y. Fujita, K. Murase, M. Nakamura, and S. Itagaki for technical support. We thank Drs. T Tsuboi and K. Tanabe for their kind support and for providing critical reagents, such as *Pf*MSP1. This study was supported by grants from the Ministry of Education, Culture, Sports, Science and Technology in Japan; from the RT Fund for Technology Development and CREST, JST, Japan; and from the National Institutes of Health. T.R. was supported by a fellowship from the Swiss National Science Foundation. C.C, T.T, K.J.I., and S.A. filed a patent application related to the method and usage of hemozoin as an adjuvant. Y.I., K.O., and T.T. are employees for Nihon ZENOAQ, which develops GMP lot of hemozoin, and were funded by JST.

Received: July 29, 2009
Revised: October 20, 2009
Accepted: December 7, 2009
Published: January 20, 2010

REFERENCES

Aoki, S., Li, J., Itagaki, S., Okech, B.A., Egwang, T.G., Matsuoka, H., Palacpac, N.M., Mitamura, T., and Horii, T. (2002). Serine repeat antigen (SERA5) is predominantly expressed among the SERA multigene family of Plasmodium falciparum, and the acquired antibody titers correlate with serum inhibition of the parasite growth. J. Biol. Chem. *277*, 47533–47540.

Arese, P., and Schwarzer, E. (1997). Malarial pigment (haemozoin): a very active 'inert' substance. Ann. Trop. Med. Parasitol. *91*, 501–516.

Bohle, D.S., Kosar, A.D., and Stephens, P.W. (2002). Phase homogeneity and crystal morphology of the malaria pigment beta-hematin. Acta Crystallogr. D Biol. Crystallogr. *58*, 1752–1756.

Burckstummer, T., Baumann, C., Bluml, S., Dixit, E., Durnberger, G., Jahn, H., Planyavsky, M., Bilban, M., Colinge, J., Bennett, K.L., and Superti-Furga, G. (2009). An orthogonal proteomic-genomic screen identifies AIM2 as a cytoplasmic DNA sensor for the inflammasome. Nat. Immunol. *10*, 266–272.

Coban, C., Ishii, K.J., Horii, T., and Akira, S. (2007a). Manipulation of host innate immune responses by the malaria parasite. Trends Microbiol. *15*, 271–278.

Coban, C., Ishii, K.J., Kawai, T., Hemmi, H., Sato, S., Uematsu, S., Yamamoto, M., Takeuchi, O., Itagaki, S., Kumar, N., et al. (2005). Toll-like receptor 9 mediates innate immune activation by the malaria pigment hemozoin. J. Exp. Med. *201*, 19–25.

Coban, C., Ishii, K.J., Uematsu, S., Arisue, N., Sato, S., Yamamoto, M., Kawai, T., Takeuchi, O., Hisaeda, H., Horii, T., and Akira, S. (2007b). Pathological role of Toll-like receptor signaling in cerebral malaria. Int. Immunol. *19*, 67–79.

Coppel, R.L. (2009). Vaccinating with the genome: a Sisyphean task? Trends Parasitol. *25*, 67–79.

Delaglio, F., Grzesiek, S., Vuister, G.W., Zhu, G., Pfeifer, J., and Bax, A. (1995). NMRPipe: a multidimensional spectral processing system based on UNIX pipes. J. Biomol. NMR *6*, 277–293.

Doolan, D.L., Dobano, C., and Baird, J.K. (2009). Acquired immunity to malaria. Clin. Microbiol. Rev. *22*, 13–36.

Dostert, C., Guarda, G., Romero, J.F., Menu, P., Gross, O., Tardivel, A., Suva, M.L., Stehle, J.C., Kopf, M., Stamenkovic, I., et al. (2009). Malarial hemozoin is a Nalp3 inflammasome activating danger signal. PLoS ONE *4*, e6510.

Egan, T.J. (2008). Recent advances in understanding the mechanism of hemozoin (malaria pigment) formation. J. Inorg. Biochem. *102*, 1288–1299.

Engwerda, C.R., and Good, M.F. (2005). Interactions between malaria parasites and the host immune system. Curr. Opin. Immunol. *17*, 381–387.

Fernandes-Alnemri, T., Yu, J.W., Datta, P., Wu, J., and Alnemri, E.S. (2009). AIM2 activates the inflammasome and cell death in response to cytoplasmic DNA. Nature *458*, 509–513.

Franchi, L., Eigenbrod, T., Munoz-Planillo, R., and Nunez, G. (2009). The inflammasome: a caspase-1-activation platform that regulates immune responses and disease pathogenesis. Nat. Immunol. *10*, 241–247.

Franchi, L., and Nunez, G. (2008). The Nlrp3 inflammasome is critical for aluminium hydroxide-mediated IL-1beta secretion but dispensable for adjuvant activity. Eur. J. Immunol. *38*, 2085–2089.

Franklin, B.S., Parroche, P., Ataide, M.A., Lauw, F., Ropert, C., de Oliveira, R.B., Pereira, D., Tada, M.S., Nogueira, P., da Silva, L.H., et al. (2009). Malaria primes the innate immune response due to interferon-gamma induced enhancement of toll-like receptor expression and function. Proc. Natl. Acad. Sci. USA *106*, 5789–5794.

Girard, M.P., Reed, Z.H., Friede, M., and Kieny, M.P. (2007). A review of human vaccine research and development: malaria. Vaccine *25*, 1567–1580.

Good, M.F. (2009). The hope but challenge for developing a vaccine that might control malaria. Eur. J. Immunol. *39*, 939–943.

Griffith, J.W., O'Connor, C., Bernard, K., Town, T., Goldstein, D.R., and Bucala, R. (2007). Toll-like receptor modulation of murine cerebral malaria is dependent on the genetic background of the host. J. Infect. Dis. *196*, 1553–1564.

Griffith, J.W., Sun, T., McIntosh, M.T., and Bucala, R. (2009). Pure Hemozoin is inflammatory in vivo and activates the NALP3 inflammasome via release of uric acid. J. Immunol. *183*, 5208–5220.

Hanscheid, T., Egan, T.J., and Grobusch, M.P. (2007). Haemozoin: from melatonin pigment to drug target, diagnostic tool, and immune modulator. Lancet Infect. Dis. *7*, 675–685.

Hisaeda, H., Tetsutani, K., Imai, T., Moriya, C., Tu, L., Hamano, S., Duan, X., Chou, B., Ishida, H., Aramaki, A., et al. (2008). Malaria parasites require TLR9 signaling for immune evasion by activating regulatory T cells. J. Immunol. *180*, 2496–2503.

Hornung, V., Ablasser, A., Charrel-Dennis, M., Bauernfeind, F., Horvath, G., Caffrey, D.R., Latz, E., and Fitzgerald, K.A. (2009). AIM2 recognizes cytosolic dsDNA and forms a caspase-1-activating inflammasome with ASC. Nature *458*, 514–518.

Hou, C.C., Day, M.J., Nuttall, T.J., and Hill, P.B. (2006). Evaluation of IgG subclass responses against Dermatophagoides farinae allergens in healthy and atopic dogs. Vet. Dermatol. *17*, 103–110.

Ishii, K.J., Koyama, S., Nakagawa, A., Coban, C., and Akira, S. (2008). Host innate immune receptors and beyond: making sense of microbial infections. Cell Host Microbe *3*, 352–363.

Jaramillo, M., Bellemare, M.J., Martel, C., Shio, M.T., Contreras, A.P., Godbout, M., Roger, M., Gaudreault, E., Gosselin, J., Bohle, D.S., and Olivier, M. (2009). Synthetic Plasmodium-like hemozoin activates the immune response: a morphology - function study. PLoS ONE *4*, e6957.

Jaramillo, M., Godbout, M., and Olivier, M. (2005). Hemozoin induces macrophage chemokine expression through oxidative stress-dependent and -independent mechanisms. J. Immunol. *174*, 475–484.

Kaisho, T., and Akira, S. (2002). Toll-like receptors as adjuvant receptors. Biochim. Biophys. Acta *1589*, 1–13.

Keller, C.C., Yamo, O., Ouma, C., Ong'echa, J.M., Ounah, D., Hittner, J.B., Vulule, J.M., and Perkins, D.J. (2006). Acquisition of hemozoin by monocytes down-regulates interleukin-12 p40 (IL-12p40) transcripts and circulating IL-12p70 through an IL-10-dependent mechanism: in vivo and in vitro findings in severe malarial anemia. Infect. Immun. *74*, 5249–5260.

Kongkasuriyachai, D., Fujioka, H., and Kumar, N. (2004). Functional analysis of Plasmodium falciparum parasitophorous vacuole membrane protein (Pfs16) during gametocytogenesis and gametogenesis by targeted gene disruption. Mol. Biochem. Parasitol. *133*, 275–285.

Krishnegowda, G., Hajjar, A.M., Zhu, J., Douglass, E.J., Uematsu, S., Akira, S., Woods, A.S., and Gowda, D.C. (2005). Induction of proinflammatory responses in macrophages by the glycosylphosphatidylinositols of Plasmodium falciparum: cell signaling receptors, glycosylphosphatidylinositol (GPI) structural requirement, and regulation of GPI activity. J. Biol. Chem. *280*, 8606–8616.

Latz, E., Verma, A., Visintin, A., Gong, M., Sirois, C.M., Klein, D.C., Monks, B.G., McKnight, C.J., Lamphier, M.S., Duprex, W.P., et al. (2007). Ligand-induced conformational changes allosterically activate Toll-like receptor 9. Nat. Immunol. *8*, 772–779.

Lepenies, B., Cramer, J.P., Burchard, G.D., Wagner, H., Kirschning, C.J., and Jacobs, T. (2008). Induction of experimental cerebral malaria is independent of TLR2/4/9. Med. Microbiol. Immunol. *197*, 39–44.

Martinon, F., Petrilli, V., Mayor, A., Tardivel, A., and Tschopp, J. (2006). Gout-associated uric acid crystals activate the NALP3 inflammasome. Nature *440*, 237–241.

McGee, J.P., Singh, M., Li, X.M., Qiu, H., and O'Hagan, D.T. (1997). The encapsulation of a model protein in poly (D, L lactide-co-glycolide) microparticles of various sizes: an evaluation of process reproducibility. J. Microencapsul. *14*, 197–210.

Muruve, D.A., Petrilli, V., Zaiss, A.K., White, L.R., Clark, S.A., Ross, P.J., Parks, R.J., and Tschopp, J. (2008). The inflammasome recognizes cytosolic microbial and host DNA and triggers an innate immune response. Nature *452*, 103–107.

Okech, B., Mujuzi, G., Ogwal, A., Shirai, H., Horii, T., and Egwang, T.G. (2006). High titers of IgG antibodies against Plasmodium falciparum serine repeat antigen 5 (SERA5) are associated with protection against severe malaria in Ugandan children. Am. J. Trop. Med. Hyg. *74*, 191–197.

Orengo, J.M., Evans, J.E., Bettiol, E., Leliwa-Sytek, A., Day, K., and Rodriguez, A. (2008). Plasmodium-induced inflammation by uric acid. PLoS Pathog. *4*, e1000013.

Pagola, S., Stephens, P.W., Bohle, D.S., Kosar, A.D., and Madsen, S.K. (2000). The structure of malaria pigment beta-haematin. Nature *404*, 307–310.

Palm, N.W., and Medzhitov, R. (2009). Pattern recognition receptors and control of adaptive immunity. Immunol. Rev. *227*, 221–233.

Parroche, P., Lauw, F.N., Goutagny, N., Latz, E., Monks, B.G., Visintin, A., Halmen, K.A., Lamphier, M., Olivier, M., Bartholomeu, D.C., et al. (2007). Malaria hemozoin is immunologically inert but radically enhances innate responses by presenting malaria DNA to Toll-like receptor 9. Proc. Natl. Acad. Sci. USA *104*, 1919–1924.

Pichyangkul, S., Yongvanitchit, K., Kum-arb, U., Hemmi, H., Akira, S., Krieg, A.M., Heppner, D.G., Stewart, V.A., Hasegawa, H., Looareesuwan, S., et al. (2004). Malaria blood stage parasites activate human plasmacytoid dendritic cells and murine dendritic cells through a Toll-like receptor 9-dependent pathway. J. Immunol. *172*, 4926–4933.

Pombo, D.J., Lawrence, G., Hirunpetcharat, C., Rzepczyk, C., Bryden, M., Cloonan, N., Anderson, K., Mahakunkijcharoen, Y., Martin, L.B., Wilson, D., et al. (2002). Immunity to malaria after administration of ultra-low doses of red cells infected with Plasmodium falciparum. Lancet *360*, 610–617.

Pulendran, B., and Ahmed, R. (2006). Translating innate immunity into immunological memory: implications for vaccine development. Cell *124*, 849–863.

Reed, S.G., and Scott, P. (1993). T-cell and cytokine responses in leishmaniasis. Curr. Opin. Immunol. *5*, 524–531.

Roberts, T.L., Idris, A., Dunn, J.A., Kelly, G.M., Burnton, C.M., Hodgson, S., Hardy, L.L., Garceau, V., Sweet, M.J., Ross, I.L., et al. (2009). HIN-200 proteins regulate caspase activation in response to foreign cytoplasmic DNA. Science *323*, 1057–1060.

Rutz, M., Metzger, J., Gellert, T., Luppa, P., Lipford, G.B., Wagner, H., and Bauer, S. (2004). Toll-like receptor 9 binds single-stranded CpG-DNA in a sequence- and pH-dependent manner. Eur. J. Immunol. *34*, 2541–2550.

Schofield, L., Hewitt, M.C., Evans, K., Siomos, M.A., and Seeberger, P.H. (2002). Synthetic GPI as a candidate anti-toxic vaccine in a model of malaria. Nature *418*, 785–789.

Seixas, E., Moura Nunes, J.F., Matos, I., and Coutinho, A. (2009). The interaction between DC and Plasmodium berghei/chabaudi-infected erythrocytes in mice involves direct cell-to-cell contact, internalization and TLR. Eur. J. Immunol. *39*, 1850–1863.

Snounou, G., Viriyakosol, S., Zhu, X.P., Jarra, W., Pinheiro, L., do Rosario, V.E., Thaithong, S., and Brown, K.N. (1993). High sensitivity of detection of human malaria parasites by the use of nested polymerase chain reaction. Mol. Biochem. Parasitol. *61*, 315–320.

Stevenson, M.M., and Riley, E.M. (2004). Innate immunity to malaria. Nat. Rev. Immunol. *4*, 169–180.

Su, Z., Tam, M.F., Jankovic, D., and Stevenson, M.M. (2003). Vaccination with novel immunostimulatory adjuvants against blood-stage malaria in mice. Infect. Immun. *71*, 5178–5187.

Takeshita, F., and Ishii, K.J. (2008). Intracellular DNA sensors in immunity. Curr. Opin. Immunol. *20*, 383–388.

Togbe, D., Schofield, L., Grau, G.E., Schnyder, B., Boissay, V., Charron, S., Rose, S., Beutler, B., Quesniaux, V.F., and Ryffel, B. (2007). Murine cerebral malaria development is independent of toll-like receptor signaling. Am. J. Pathol. *170*, 1640–1648.

Xiang, S.D., Scholzen, A., Minigo, G., David, C., Apostolopoulos, V., Mottram, P.L., and Plebanski, M. (2006). Pathogen recognition and development of particulate vaccines: does size matter? Methods *40*, 1–9.

INFECTIOUS DISEASE

Plasmacytoid Dendritic Cells Delineate Immunogenicity of Influenza Vaccine Subtypes

Shohei Koyama,[1,2] Taiki Aoshi,[3] Takeshi Tanimoto,[4] Yutaro Kumagai,[1] Kouji Kobiyama,[3] Takahiro Tougan,[3] Kazuo Sakurai,[5] Cevayir Coban,[1] Toshihiro Horii,[3] Shizuo Akira,[1]* Ken J. Ishii[1,3]*

(Published 31 March 2010; Volume 2 Issue 25 25ra24)

A variety of different vaccine types are available for H1N1 influenza A virus infections; however, their immunological mechanisms of action remain unclear. Here, we show that plasmacytoid dendritic cells (pDCs) and type I interferon (IFN)–mediated signaling delineate the immunogenicity of live attenuated virus, inactivated whole-virus (WV), and split virus vaccines. Although Toll-like receptor 7 acted as the adjuvant receptor for the immunogenicity of both live virus and WV vaccines, the requirement for type I IFN production by pDCs for the immunogenicity of the vaccines was restricted to WV. A split vaccine commonly used in humans failed to immunize naïve mice, but a pDC-activating adjuvant could restore immunogenicity. In blood from human adults, however, split vaccine alone could recall memory T cell responses, underscoring the importance of this adjuvant pathway for primary, but not secondary, vaccination.

INTRODUCTION

Vaccination is considered to be the best prophylaxis for influenza virus infection (*1*). There are three different types of influenza virus vaccines: live attenuated influenza virus (LAIV), formalin-inactivated whole-virus (WV) vaccine, and ether-treated hemagglutinin (HA) antigen–enriched virion-free "split" virus (SV) or "subunit" virus (SU) vaccine (*2*). Among them, SV and SU are the most commonly used in clinics because there are fewer reactogenicities, although LAIV and WV have been shown to have superior immunogenicity, especially in children (*3–5*). The immunogenicity and efficacy of these vaccines can be affected by host factors, such as age and immunological status [such as immunodeficiency (*6–8*)], and viral factors, including the antigenic mismatch between the vaccines and the circulating virus strains (*9*). However, the exact mechanisms used by the three types of vaccine compositions to achieve immunogenicity and how these mechanisms differ are not fully understood.

It is known that most, if not all, successful vaccines that induce strong protection against pathogens contain adjuvant components that activate the innate immune system via specific receptors, including Toll-like receptors (TLRs), retinoic acid–inducible gene-I (RIG-I)–like receptors (RLRs), and Nod-like receptors (NLRs) (*10–12*). These receptors are expressed by antigen-presenting cells, such as dendritic cells (DCs), which mediate the subsequent adaptive immune response by releasing specific cytokines, such as interferons (IFNs) and interleukins (ILs), and activating antigen-specific T and B cells. The nature of the adjuvant and the specific receptors that are activated on DCs can determine the type of immune response that is generated (*10–12*). Recent studies suggest that TLR7 and a certain NLR that activates the inflammasome—a collection of components that spur the innate immune system—are involved in controlling adaptive immune responses to influenza A virus infection (*13*, *14*). Our previous work has characterized a key role for TLR signaling in the immune response to inactivated WV vaccination (*13*); however, no comprehensive study directly compares the role of TLRs, NLRs, and RLRs in either live virus or inactivated WV vaccinations (*15*). Here, we decipher the mechanism(s) by which the various virus preparations drive development of immunogenicity.

[1]Laboratory of Host Defense, WPI Immunology Frontier Research Center, Osaka University, Suita, Osaka 565–0871, Japan. [2]Department of Respiratory Medicine, Tohoku University Graduate School of Medicine, Sendai, Miyagi 980–8575, Japan. [3]Department of Molecular Protozoology, Research Institute for Microbial Diseases, Osaka University, Suita, Osaka 565–0871, Japan. [4]The Research Foundation for Microbial Diseases of Osaka University, Kan-on-ji, Kagawa 768–0061, Japan. [5]Department of Chemical Processes and Environments, University of Kitakyushu, Kitakyushu, Fukuoka 808–0135, Japan.
*To whom correspondence should be addressed. E-mail: kenishii@biken.osaka-u.ac.jp (K.J.I.); sakira@biken.osaka-u.ac.jp (S.A.)

RESULTS

Inactivated WV requires TLR7-mediated, but not RLR- or NLR-mediated, immune activation for its immunogenicity

We first examined whether an inactivated WV preparation of the A/New Caledonia/20/1999 (NC) (H1N1) strain can immunize mice lacking TLR7, IPS-1 (IFN-β promoter stimulator–1; an adaptor protein for RIG-I–mediated type I IFN production), and ASC (apoptotic speck protein; containing a caspase recruitment domain, an adaptor molecule required for NLRP3 inflammasome activation). All three of these genes have been shown to be involved in innate immune recognition of live influenza virus infection (*14*, *16–19*).

We immunized TLR7-deficient or IPS-1–deficient mice intranasally (i.n.) with WV of NC H1N1 twice at a 2-week interval. One week after the second injection, the vaccination-induced, virus-specific B cell and $CD4^+$ T cell adaptive immune responses were analyzed. TLR7-deficient mice showed virtually no virus-specific immunoglobulin A (IgA) in bronchoalveolar lavage fluid (BALF), no virus-specific IgG in serum (Fig. 1A), and no IFN-γ production from $CD4^+$ T cells specific to a viral nucleoprotein (NP) antigen epitope ($NP_{260–283}$ specific to $I\text{-}A^b$) (Fig. 1B), whereas IPS-1–deficient mice mounted comparable levels of these responses to wild-type mice (Fig. 1, A and B). Consistently, the immunized TLR7-deficient mice were not protected against a lethal challenge with the A/Puerto Rico/8/34 (PR) (H1N1) strain, whereas the immunized IPS-1–deficient mice were protected to a level comparable to vaccinated wild-type mice (Fig. 1C). We

obtained similar results with intramuscular (i.m.) immunization of these mice, with respect to total IgG titer and IgG2a titer (fig. S1). In contrast to i.n. immunization, i.m. immunization failed to elicit BALF IgA in either wild-type or TLR7-deficient mice. There was an enhanced serum IgG1 response in TLR7-deficient mice relative to wild-type mice, but this response failed to protect the TLR7-deficient mice from lethal challenge with PR H1N1 (fig. S1, A and C). Thus, the inactivated WV vaccine requires TLR7-mediated, but not RIG-I–mediated, IPS-1 for its immunogenicity, which is consistent with findings for the live virus vaccination (*13*).

We also immunized ASC-deficient mice with WV (NC H1N1) because a role for the ASC inflammasome in the adaptive immune response to influenza virus infection is controversial (*14*, *19*). ASC-deficient mice did not show any defects in their adaptive immune responses to WV immunization relative to wild-type mice (Fig. 1, D and E). Notably, ASC was not involved in the immunogenicity of live virus immunization, except for serum IgG1 production, whereas $CD8^+$ T cell responses were not observed with WV immunization (fig. S2). Immunized wild-type and ASC-deficient mice were similarly protected against lethal PR H1N1 virus challenge relative to naïve wild-type mice (Fig. 1F). Therefore, ASC inflammasome activation was not essential for the induction of virus-specific B and CD4 T cell responses to WV.

The type I IFN receptor is important for the immunogenic response to inactivated WV vaccine but not to the live virus

Because both the inactivated WV and the live virus require TLR7 for their immunogenicity, we sought to identify the downstream effector molecule(s) involved. Type I IFNs, such as IFN-α and IFN-β, are known to have potent adjuvant activity (*20*, *21*), and a recent study showed that WV immunization substantially up-regulated the expression of IFN-inducible genes, such as *Cxcl10* (*22*). Therefore, as a systemic indicator of type I IFN responses, we examined the amounts of the cytokine CXCL10 in the sera of mice 24 hours after vaccination. The induction of CXCL10 was significantly reduced in TLR7-deficient mice relative to wild-type, IPS-1–deficient, and ASC-deficient mice (Fig. 2A). Similar results were obtained for messenger RNA (mRNA) analyses of IFN-β and CXCL10 in the lung (fig. S3A), suggesting that type I IFNs might be dominant effector molecules in this TLR7-dependent system. To test this hypothesis directly, we i.n. immunized mice deficient in the IFN-α and IFN-β receptor 2 (IFNAR2) with WV as in Fig. 1. IFNAR2-deficient mice failed to induce virus-specific antibodies (including BALF IgA and serum IgG) and $CD4^+$ T cell responses (Fig. 2B and fig. S3, B and C) relative to the heterozygous IFNAR2 knockout mice. As a result, mortality was increased and a significantly larger body weight loss was observed after lethal PR H1N1 challenge in the IFNAR2-deficient mice (Fig. 2C). Naïve wild-type and IFNAR2-deficient mice showed similar susceptibilities to PR H1N1 challenge, consistent with a previous study (*23*). Similar results were also observed after i.m. immunization (fig. S3, D and E). When naïve IFNAR2-deficient mice were immunized with live virus, there was no alteration of the virus-specific serum IgG and IFN-γ secretion by virus NP antigen-specific $CD4^+$ T cells ($NP_{260–283}$ specific to $I\text{-}A^b$) and $CD8^+$ T cells ($NP_{366–374}$ specific to $H\text{-}2D^b$) (fig. S3, F to I), consistent with a previous study (*23*). Together, these results suggest that TLR7, but not RLRs or NLRs, is required for immunogenicity of inactivated as well as live influenza virus vaccination. In addition, the type I IFN receptor–mediated signaling pathway was critical for the immunogenic response to WV but not to the live virus.

Live virus and inactivated WV vaccines induce type I IFNs through distinct DC types

DCs are a critical component of the innate immune system that recognize vaccines and mediate the adaptive immune response. There are different subtypes of DCs that can be divided loosely into conventional myeloid DCs (mDCs) and plasmacytoid DCs (pDCs), which express different receptors and secrete different cytokines on activation. To characterize in more detail the immune response triggered by the WV vaccine and live virus, we stimulated two types of bone marrow–derived DCs—Flt3

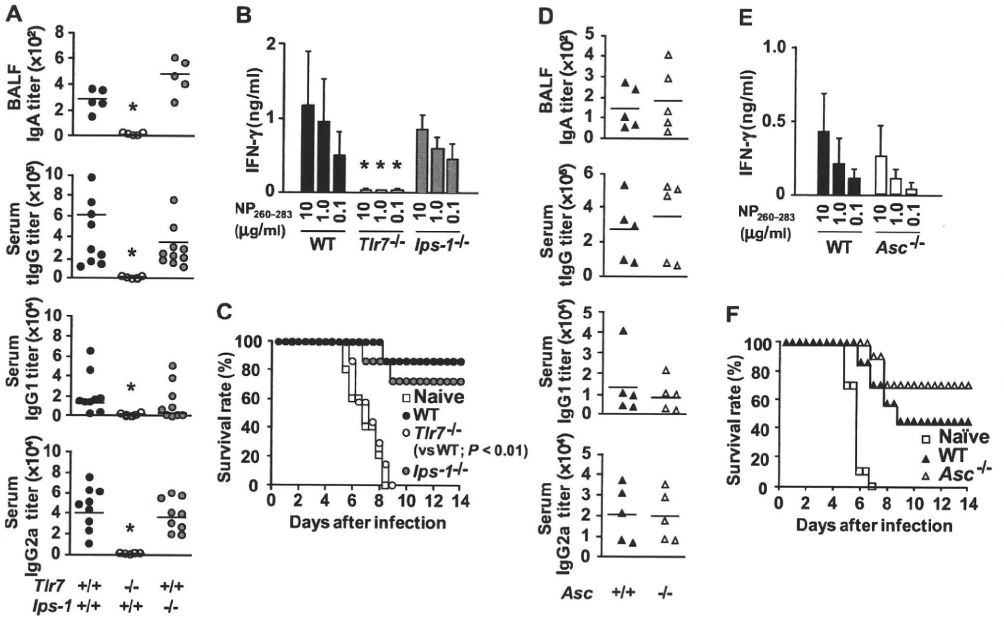

Fig. 1. TLR7-dependent, but not IPS-1–dependent or ASC-dependent, signaling is required for the induction of protective immune responses by inactivated WV. (**A** to **C**) Wild-type (WT), *Tlr7*-deficient, and *Ips-1*–deficient mice ($n = 9$ per group) were i.n. vaccinated with WV of NC (1.5 μg per mouse) twice, with a 2-week interval. One week after the second vaccination, we measured titers of antigen-specific mucosal (BALF) IgA and serum total IgG (tIgG), IgG1, and IgG2a (A) and IFN-γ production by $CD4^+$ T cells (B) by ELISA as described in Materials and Methods. *$P < 0.05$ versus WT mice. (C) Vaccinated mice ($n = 9$ per group) were challenged with $10 \times LD_{50}$ (median lethal dose) (2×10^4 PFU per mouse) of lethal influenza virus PR, and their survival was monitored. *$P < 0.05$ versus vaccinated WT mice. (**D** to **F**) WT and *Asc*-deficient mice ($n = 5$, each group) were similarly vaccinated, and their antigen-specific antibody responses (D), IFN-γ production by $CD4^+$ T cells (E), and survival (WT, $n = 7$; *Asc*-deficient, $n = 10$; naïve, $n = 10$) (F) were determined by ELISA as described in Materials and Methods. Each bar represents the mean (A and D) or mean ± SD (B and E). These results are representative of two independent experiments.

ligand–generated DCs (FL-DCs; which contain pDCs) and granulocyte-macrophage colony-stimulating factor (GM-CSF)–generated DCs (GM-DCs; which contain conventional DCs but no pDCs)—with the live virus or WV and then measured their IFN-β production by enzyme-linked immunosorbent assay (ELISA). The live virus strongly stimulated FL-DCs to produce IFN-β in a TLR7-dependent manner, whereas production by GM-DCs was in a TLR7-independent manner (Fig. 2D), consistent with our previous study (*13*). In contrast, WV-activated FL-DCs, but not GM-DCs, produced IFN-β, a process entirely dependent on TLR7 signaling (Fig. 2D), indicating that there is a clear distinction between the live virus and WV in terms of their abilities to activate DCs to secrete type I IFNs.

To confirm these in vitro observations in vivo, we next depleted pDCs in vivo to examine the role of these cells in the induction of adaptive immune responses to live virus and WV, as pDCs are known to play a key role in bridging the innate and adaptive immune responses (*24*). Wild-type mice were treated intravenously with an antibody to mPDCA-1 (*25*) and then immunized 24 hours later with the live virus or WV. Depletion of pDCs was confirmed in the spleen (fig. S4). After live virus vaccination, the concentrations of mRNAs derived from genes involved in induction of the adaptive immune response, specifically *Ifnb*, *Cxcl10*, *Il6*, and *Ccl2*, were clearly elevated in the lung irrespective of treatment with antibody to mPDCA-1 (Fig. 2E). In contrast, these transcriptional responses were severely impaired after WV vaccination in pDC-depleted mice relative to isotype control antibody–treated mice (Fig. 2E). Serum CXCL10 was also reduced in pDC-depleted mice treated with WV but not the live virus (Fig. 2F). Thus, both live virus and WV induced type I IFNs predominantly through pDCs in vivo; however, WV was dominantly recognized by pDCs, whereas live virus could also stimulate other cell types to activate innate immune responses.

Although it was previously reported that pDC activation is not essential for the induction of adaptive immune responses in live influenza virus infection (*26*, *27*), pDC depletion specifically rendered the inactivated WV nonimmunogenic, as measured by virus-specific IgG concentrations in serum (Fig. 3A). In these experiments, mice were treated with an antibody to mPDCA-1 twice at both the primary and the secondary vaccinations. To further examine the more detailed role of pDCs in the primary and/or secondary vaccinations, we treated mice with an antibody to mPDCA-1 at either the primary or the secondary (boost) vaccination. Virus-specific mucosal IgA, serum IgG (Fig. 3B), and $CD4^+$ T cell IFN-γ (Fig. 3C) were significantly impaired when pDCs were depleted in the primary, but not in the secondary, vaccination with the inactivated WV. Thus, pDC activation is essential for inducing B cell and $CD4^+$ T cell responses to the inactivated WV during primary, but not secondary, vaccination. By sharp contrast, pDC activation at priming was not required for inducing B cell and $CD4^+$ T cell responses with the live virus.

WV-loaded pDCs were sufficient to transfer immunogenicity to naïve mice, which requires intrinsic as well as extrinsic type I IFN signaling

To further examine the role of pDCs, we performed cell transfer experiments. FL-DCs from wild-type mice were separated into two populations, namely, a B220 (CD45R)–enriched population containing pDCs and a B220-depleted population containing virtually no pDCs (as indicated in Fig. 3D). The cell populations were pulsed with WV and injected intravenously into wild-type mice. The virus-specific IgG concentrations elicited by the B220-enriched FL-DCs were significantly higher than those elicited by the B220-depleted population (Fig. 3D). In addition, when we transferred B220-enriched FL-DCs derived from the IFNAR2-deficient mice (lacking type I IFN) into wild-type mice or vice versa, virus-specific IgG induction was significantly impaired in both cases (Fig. 3E). We also confirmed that IFNAR2-deficient FL-DCs secreted significantly less type I IFN relative to that of FL-DCs from the heterozygous IFNAR2 knockout mice (fig. S5A). When we tested TLR7 deficiency with

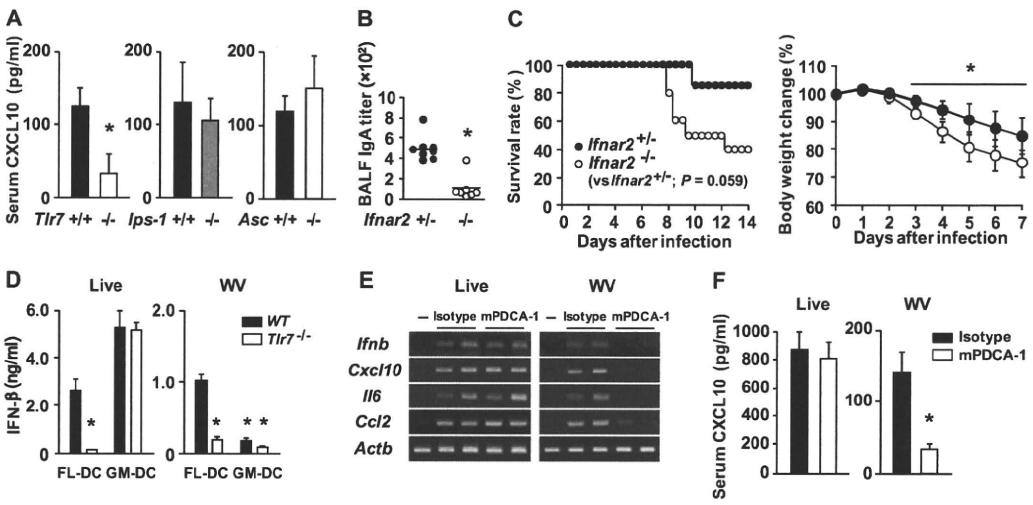

Fig. 2. Critical roles of type I IFN receptor–mediated signaling and pDC activation in inducing adaptive immune responses to the inactivated WV vaccine but not to the live virus. (**A**) *Tlr7*-deficient, *Ips-1*–deficient, *Asc*-deficient, and control mice ($n = 3$ per group) were i.n. vaccinated with WV (3.0 μg per mouse), and CXCL10 production in sera was measured by ELISA after 24 hours. *$P < 0.05$ versus control mice. (**B** and **C**) Control ($Ifnar2^{+/-}$) and type I IFN receptor–deficient ($Ifnar2^{-/-}$) mice ($n = 8$, each group) were i.n. vaccinated with WV (1.5 μg per mouse) as in Fig. 1, and BALF IgA (B) was measured by ELISA. *$P < 0.05$ versus control mice. The mice were then infected with lethal influenza PR at $10 \times LD_{50}$, and their survival and body weight (C) were monitored. *$P < 0.05$ versus control mice. (**D**) Type I IFN production by FL-DCs and GM-DCs from WT and *Tlr7*-deficient mice in response to the live virus [multiplicity of infection (MOI) = 10] and WV (5 μg/ml). IFN-β production was measured by ELISA 24 hours after the stimulation. *$P < 0.05$ versus WT FL-DC. (**E** and **F**) Innate immune responses to WV in pDC-depleted mice. Mice were treated with an antibody to mPDCA-1 24 hours before inoculation and then i.n. challenged with the live virus (1×10^5 PFU per mouse) or WV vaccine (5 μg per mouse). The expression of IFN-β, CXCL10, IL-6, and CCL2 mRNA in the lungs (E) and CXCL10 in sera (F) 24 hours after vaccination was measured by RT-PCR and ELISA. *$P < 0.05$ versus control mice. These results are representative of at least two independent experiments.

the same approach, we observed a substantial TLR7 signaling dependency in these FL-DC transfer experiments (fig. S5B). These results suggest that type I IFN–mediated signaling in pDCs, as well as in the recipient as yet unidentified cell type(s), is indispensable for eliciting the adaptive immune response to WV.

Split vaccine does not protect naïve mice, but immunogenicity can be improved with a pDC-activating adjuvant while it recalls memory T cells in human adult blood

Currently, the most widely used influenza vaccines in many countries comprise SV or SU, which mainly consist of purified protein antigens such as HA and neuraminidase. As mentioned earlier, vaccination of mice with SV led to significantly lower production of type I IFNs and related chemokines, such as CXCL10, at both the mRNA and the protein levels in the lung and serum, respectively (Fig. 4, A and B). SV also failed to activate DCs to produce type I IFNs in vitro (fig. S6A). These data suggest that the intrinsic TLR7 ligand (that is, viral genomic RNA) was lost during the SV production process. In support of this idea, removal of the RNA content from WV by ribonuclease treatment significantly decreased the TLR7-mediated type I IFN production by pDCs (fig. S6B). The reduced immunostimulatory activity of SV was associated with its diminished immunogenicity. When naïve mice were immunized with SV at the same dose, adjusted to the HA content (fig. S6C), as WV, the HA-specific IgG and CD4 T cell responses were significantly lower than those elicited by WV (Fig. 4, C and D). Together, these data strongly suggest that SV loses its built-in TLR7 adjuvant (viral genome RNA) during purification of WV, consistent with a recent study for the H5N1 virus (*28*).

Our results thus far raise the possibility of improving SV immunogenicity by adding a pDC-activating TLR ligand. Because pDCs express both TLR7 and TLR9, we examined whether addition of a TLR9 ligand to the "adjuvant-lost" split vaccine would replace the natural TLR7-mediated pDC activation. We used a second-generation TLR9 ligand of CpG DNA complexed with β-(1→3)-D-glucan, namely, schizophyllan (SPG) (*29*). This new TLR9 ligand is more potent and durable than naked CpG DNA, and it still retains the TLR9 ligand activity. Mice were i.n. immunized with WV, SV, or SV plus the SPG-CpG DNA conjugate (SV+SPG-CpG) and then evaluated for their adaptive immune responses. The SV+SPG-CpG induced robust type I IFN responses independently of TLR7 (Fig. 4, A and B). Correspondingly, the SV+SPG-CpG successfully enhanced HA-specific B cell and $CD4^+$ T cell responses to levels comparable to those from WV immunization of wild-type mice (Fig. 4, C and D). Immunization of TLR9-deficient mice provided further evidence that the responses induced by the SV+SPG-CpG were dependent on TLR9 but not on TLR7 (fig. S7A).

The protective efficacies of these three types of vaccines were also examined in mice. WV conferred protection against lethal PR H1N1 virus challenge in a TLR7-dependent and TLR9-independent manner, whereas the SV+SPG-CpG provided protection in a TLR9-dependent and TLR7-independent manner (Fig. 4E and fig. S7B). Notably, the original SV failed to provide protection against lethal PR H1N1 virus challenge in any of the groups of mice examined (Fig. 4E and fig. S7B). We also confirmed that the restored protective effect of the SPG-CpG adjuvant was mediated by type I IFN responses because IFNAR2-deficient mice failed to mount virus-specific B and T cell responses (fig. S7, C and D) and demonstrated no improved protection against infection (fig. S7E).

Although the usefulness of SV vaccination in the healthy adult human population has been recognized in many studies, our results are somewhat contradictory. Therefore, we tested the relevance of these observations in a human system. Human peripheral blood mononuclear cells (PBMCs) from healthy volunteers were stimulated with H1N1 live virus, inactivated H1N1 WV, and H1N1 SV for 24 hours, and then IFN-α and IFN-γ secretion was measured by ELISA. Consistent with the mice data, IFN-α was secreted with live virus and WV but not with SV stimulation (Fig. 4F). Depletion of pDCs with BDCA4 microbeads revealed that this IFN-α secretion was totally dependent on pDC in WV and partially in live virus stimulation (Fig. 4F). On the

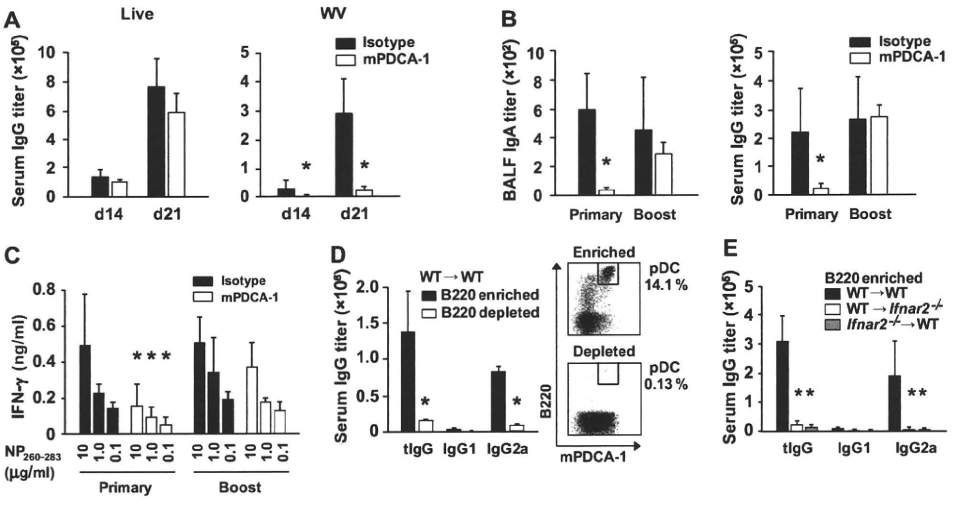

Fig. 3. Immunogenicity of the inactivated WV, but not of the live virus, depends on pDC activation at the primary vaccination. (**A**) The adaptive immune responses to WV (i.n.) were monitored in pDC-depleted mice ($n = 3$ per group). Mice were injected with an antibody to mPDCA-1 or isotype control antibody 24 hours before each vaccination, and serum IgG concentrations were measured by ELISA at the indicated times. *$P < 0.05$ versus control mice. (**B** and **C**) To determine whether pDCs are more important for priming or boosting after vaccination with inactivated WV, we treated one group of mice ($n = 3$) only with an antibody to mPDCA-1 before the primary vaccination (priming) and another group ($n = 3$) was treated only before the secondary vaccination (boosting). BALF IgA and serum IgG 1 week after the boost (B) and IFN-γ production from influenza-specific $CD4^+$ T cells (C) were measured by ELISA. *$P < 0.05$ versus control mice. (**D** and **E**) FL-DCs were separated into $B220^+$ and $B220^-$ DCs by MACS. Each DC was pulsed with WV in vitro, and $B220^+$ or $B220^-$ cells (5×10^5) were intravenously injected ($n = 3$ per group). Serum IgG was measured 2 weeks after the injection in WT mice. *$P < 0.05$ versus B220-enriched cells. (D) $B220^+$ cells (1×10^5) from WT and *Ifnar2*-deficient mice were intravenously transferred into untreated WT and *Ifnar2*-deficient mice ($n = 3$ per group), and serum IgG was measured by ELISA. *$P < 0.05$ versus WT to WT. (E) These results are representative of at least two independent experiments.

other hand, both WV and SV induced IFN-γ secretion comparably in the PBMC preparations even when the SV made from the swine-origin H1N1 A/California/04/2009 strain was used. Results obtained after $CD4^+$ and $CD8^+$ T cell depletion of the PBMC preparations revealed that virus-specific IFN-γ secretion was produced mainly by $CD4^+$ T cells in live virus and WV stimulation (Fig. 4G). These results suggest that SV could efficiently stimulate memory T cell responses without type I IFNs in a naturally (or seasonally) influenza virus–exposed human population.

DISCUSSION

Although TLR7 and certain NLRs have been shown previously to be involved in the induction of adaptive immune responses to influenza A virus infection (*13*, *14*), the current work represents a comprehensive study that directly compares the functions of TLRs, NLRs, and RLRs in the immunogenicity and efficacy of influenza inactivated WV vaccinations (Fig. 1 and fig. S1). We identified pDCs as an innate immune cell and type I IFNs as humoral factors that are essential for the immunogenicity of the inactivated WV vaccine (Figs. 2 and 3). Although our results demonstrate an essential role for pDCs in inactivated WV vaccination, other studies have identified a redundant role for pDCs in antiviral responses to live virus vaccination such as influenza virus (*26*, *27*). In addition, although TLR7 is expressed in a variety of cell types, including B cells and macrophages, our results strongly suggest an essential role for pDCs in mediating TLR7-induced innate and adaptive immune responses to inactivated influenza WV vaccination but not to live virus vaccination.

The critical role of pDCs in vaccine priming, but not in boosting, is apparent from results of the pDC depletion study, in which pDCs were removed from mice before vaccination with inactivated WV (Fig. 3, A to C). These findings parallel our in vitro data, in which the pDC-containing FL-DC preparation, but not the mDC-dominant GM-DC preparation, responded to inactivated WV to produce type I IFNs (Fig. 2D); however, these data do not necessarily exclude the involvement of other antigen-presenting cells for either priming or boosting. For example, pDCs pulsed with inactivated WV in vitro can prime naïve mice (Fig. 3D), but the type I IFNs produced by these pDCs were required not only for stimulating the pDCs themselves but also for priming as yet unidentified cell types of the recipient mouse (Fig. 3E). This suggests that cross talk exists between pDCs and the other as yet unidentified cells via type I IFN–mediated signaling. In addition, it will be of interest to examine whether other DCs, such as mDCs, are involved in this intercellular cross talk in such a way that pDCs can transfer the flu antigens to mDCs or that pDCs can present antigens directly to T cells and/or B cells. We note the distinct regulation of type I IFN induction by inactivated WV vaccination, which differed from IFN induction by live virus vaccination. Indeed, although type I IFNs were induced by both inactivated and live virus vaccinations, inactivated WV vaccines activated only TLR7 on pDCs,

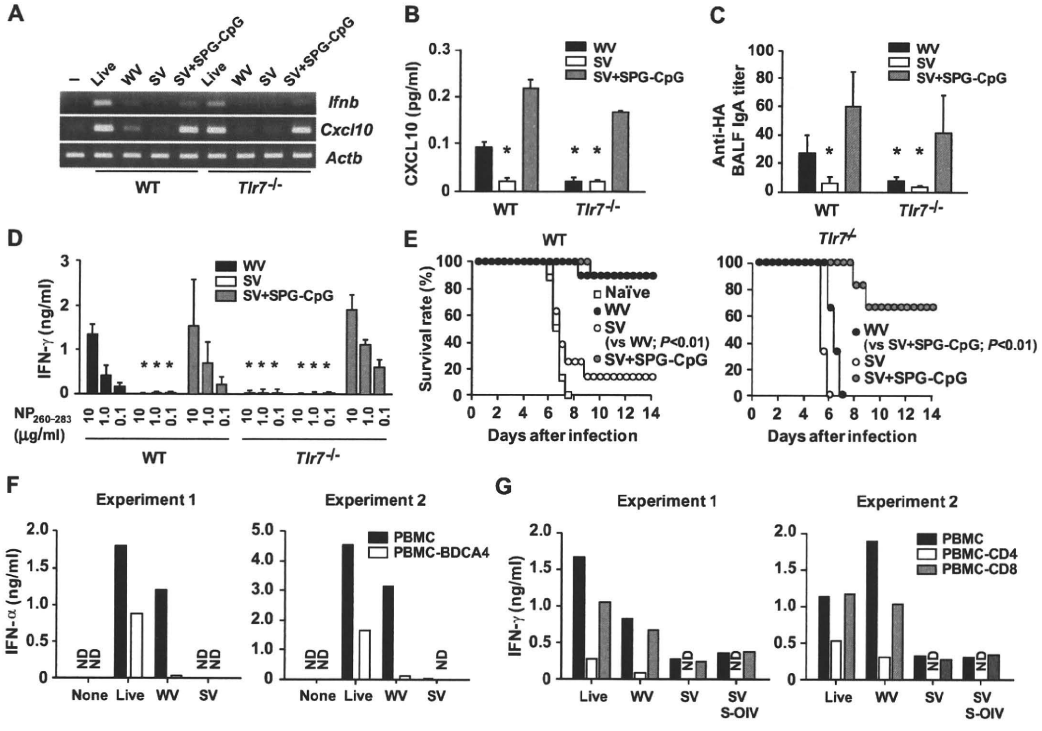

Fig. 4. Immunogenicity differences between WV and SV depend on type I IFN production via pDC activation in naïve hosts but not in primed hosts. (**A** and **B**) WT and *Tlr7*-deficient mice were i.n. vaccinated with three different vaccines as described in Materials and Methods. After 24 hours, IFN-β and CXCL10 expression in the lungs (A) and CXCL10 production in the sera (B) was measured by RT-PCR and ELISA. *$P < 0.05$ versus WT mice immunized with WV. (**C** and **D**) To compare the immunogenicities of the three vaccines, we i.n. vaccinated WT ($n = 9$) and *Tlr7*-deficient ($n = 6$) mice as described in Fig. 1 and determined antigen (HA)–specific BALF IgA, serum total IgG (C), and IFN-γ production by $CD4^+$ T cells (D) by ELISA. *$P < 0.05$ versus WT mice immunized with WV. (**E**) Vaccinated mice were challenged with the PR strain at $10 \times LD_{50}$, and their survival rates were determined as described in Materials and Methods. *$P < 0.05$ versus WT mice immunized with WV or control mice. These results are representative of at least two independent experiments. (**F** and **G**) IFN-α and IFN-γ production in response to inactivated influenza vaccines in human PBMCs. PBMCs from healthy volunteers were stimulated with live NC virus, WV, and SV. Total PBMCs and pDC-depleted PBMCs (PBMC-BDCA4) were stimulated with live NC virus (0.01 MOI), WV (1.0 μg/ml), and SV (0.5 μg/ml), and IFN-α production was measured by ELISA (F). Total PBMCs and CD4- or CD8-depleted PBMCs were stimulated with WV and SV of NC (10 and 5 μg/ml, respectively) and SV of swine-origin influenza virus (SV S-OIV) (5 μg/ml). IFN-γ production was measured by ELISA (G). These results are from 2 representatives of 10 volunteers.

whereas live virus activated both TLR7 on pDCs and other TLR7-independent pathways in the other cells, possibly mDCs (Fig. 2, D and E). Therefore, although TLR7, pDCs, and type I IFNs all were essential for inactivated WV vaccination, pDCs and type I IFNs were not essential for live virus vaccination.

The adaptor ASC is a critical component of NLRP3 inflammasome (*30*). In contrast to type I IFN responses, ASC-dependent inflammasome activation has been shown to play a critical role in the survival of the mice challenged with live influenza virus (*14*, *18*, *19*). However, the requirement for inflammasome activation to induce influenza-specific adaptive immune responses has been controversial (*14*, *19*). Our data indicate that ASC-dependent inflammasome activation is dispensable for inducing adaptive immune responses to WV and live virus, except for IgG1 production in live virus vaccination (Fig. 1 and fig. S2). Concurrent analysis comparing three innate immune signaling pathways, TLR, NLR, and RLR, enabled us to elucidate that the TLR-dependent pathway dominantly controlled the T helper 1–type protective immunity elicited by WV and live virus vaccination.

Although SV, which is now used as the first choice for influenza vaccination in many countries, was not protective in naïve mice, its decreased immunogenicity was fully restored by adding a new TLR9 ligand that stimulates pDCs to secrete type I IFNs (Fig. 4, A to E, and fig. S7). These data above further support the notion that pDC activation and their type I IFN production play a critical role in the induction of inactivated influenza vaccine immunogenicity in naïve hosts. These results might explain in part the well-known fact that the efficacy of adjuvant-less SV is lower in young children than in adults (*7*), in which SV is simply boosting the memory T and/or B cell responses. This is further supported by our results obtained using human PBMCs (Fig. 4, F and G), which suggest that most human adults have virus-specific $CD4^+$ T cells that produce IFN-γ in response not only to seasonal flu viruses but also to the novel swine H1N1 virus. Our results also indicate that memory T cells react to both internal proteins, such as those in SV, and a wide spectrum of influenza virus surface antigens, such as those on swine-origin H1N1 (*31*, *32*) and H5N1 (*33*). The age distribution of the affected population in swine-origin H1N1 and H5N1 infections, which was limited to the young, might reflect the importance of memory T cells established by recurrent exposure to seasonal influenza live viruses and vaccines (*34*, *35*)

LAIVs activate both influenza-specific IgA-secreting B cells and cytotoxic $CD8^+$ T cells (*36*), which provides certain advantages over inactivated vaccines including WV and SV. Although WV is now unavailable for seasonal influenza, it is cost-effective and can induce heterosubtypic protection not only against a challenge by H1N1 (Fig. 1C and fig. S1C) but also against H5N1 (*37*, *38*), as with LAIV (*39*). In addition, recent progress in manufacturing techniques could reduce the adverse event rate in i.m. WV immunization (*37*, *38*) to yield results that are quite different from those of past clinical trials (*3*, *40*). An i.n. WV immunization may produce a sufficient combination of efficacy, safety, and utility for both seasonal and pre-pandemic vaccines (*41*–*45*).

Together, analysis of the molecular and cellular mechanisms of different influenza vaccines provides useful information for improving vaccine immunogenicity and efficacy, as well as for choosing an appropriate form of influenza vaccine with a rational safety approach.

MATERIALS AND METHODS

Animals, cells, viruses, and reagents

The generation of *Tlr7*-, *Ips-1*–, *Ifnar2*-, and *Tlr9*-deficient mice, either on a 129/Ola × C57/BL6 or on a C57/BL6 background, has been described previously (*13*, *46*). ASC-deficient mice were a gift from V. M. Dixit (*47*).

All animal experiments were performed in accordance with the institutional guidelines for the Osaka University animal facility.

Purified influenza viruses, H1N1 (PR and NC), a recombinant HA protein of PR, and both inactivated WV and split vaccines of NC were prepared as previously described (*48*). Both types of vaccines were derived from the NC strain. Briefly, the viruses were purified from allantoic fluid by filtration (0.45 μm) followed by sedimentation through a linear sucrose gradient. For formalin-inactivated WV vaccines, purified viruses were treated with 0.1 to 0.2% formalin at 4°C for a week. For the ether-split vaccines (SV), the viruses were mixed with an equal volume of ether and then incubated for 30 min at room temperature with stirring. The mixture was centrifuged (3000 rpm, 15 min), and the aqueous phase was collected and evaporated. CpG DNA forming a triple helix with SPG, a natural polysaccharide composed of β-(1→3)-D-glucan, was used as the second-generation TLR9 ligand as previously described (*29*, *49*, *50*). DCs were prepared as described previously. Briefly, bone marrow cells were cultured in Dulbecco's modified Eagle's medium supplemented with 10% fetal calf serum, 100 mM 2-mercaptoethanol, and human Flt3 ligand (100 ng/ml) (PeproTech) or murine GM-CSF (10 ng/ml) (PeproTech) for 7 to 9 days to use as FL-DCs and GM-DCs.

Influenza virus infection and vaccination

For influenza virus infection or vaccination, mice were anesthetized and administered i.n. with 30 μl of phosphate-buffered saline (PBS) (15 μl for each nares) containing serial amount of influenza NC viruses and vaccines. Mice were infected with 1×10^5 to 2×10^5 plaque-forming units (PFU) of virus per mouse or vaccinated with WV (1.5 to 3.0 μg per mouse) or SV (0.75 μg per mouse) with or without SPG-CpG (30 μg per mouse) twice at a 2-week interval. For the analysis of protection, mice were infected with the indicated doses of lethal PR strain.

Measurement of innate immune responses

Reverse transcription polymerase chain reaction (RT-PCR) was performed to measure mRNA expression levels of type I IFNs, cytokines, and chemokines using the RNA of the stimulated cells as previously described (*13*). Protein concentrations of IFN-α, IFN-β, and CXCL10 in the culture supernatants of the stimulated cells were measured using ELISA kits (IFN-α and IFN-β, PBL Biomedical Laboratories; CXCL10, R&D Systems).

Plasmacytoid DC depletion and cell transfer

Plasmacytoid DCs were depleted by intravenous injection of antibody to mPDCA-1 (500 μg) (Miltenyi Biotec) 24 hours before live virus infection or inactivated WV vaccination.

FL-DCs were separated into two populations, B220-enriched and B220-depleted population, by B220 antibody MACS microbeads (Miltenyi Biotec) according to the manufacturer's protocol to obtain B220-enriched FL-DC. Each cell population was incubated with WV (5 to 10 μg/ml) for 3 hours, and 1×10^5 to 5×10^5 cells per mouse